The Role of Inter-Alpha-Trypsin-Inhibitor-Heavy-Chain-5 (ITIH5) in Suppressing Pancreatic Cancer Metastasis

By

Eric Douglas Young

Submitted to the graduate degree program in Cancer Biology and the Graduate Faculty of the University of Kansas in partial fulfillment of the requirements for the degree of Doctor of Philosophy.

Chair: Danny R. Welch, Ph.D.

Roy Jensen, M.D.

Nikki Cheng, Ph.D.

Tomoo Iwakuma, M.D., Ph.D.

Tim Fields, M.D., Ph.D.

Russel Swerdlow, M.D.

Michael Wolfe, Ph.D.

Date Defended: 20 April 2018

The dissertation committee for Eric D. Young certifies that this is
the approved version of the following dissertation:

The Role of Inter-Alpha-Trypsin-Inhibitor-Heavy-Chain-5 (ITIH5) in Suppressing Pancreatic Cancer Metastasis

_____

Chair: Danny R. Welch, Ph.D.

Date Approved: 20 April, 2018

Abstract

Metastasis is the spread of cancer from the site of origin to a distant site, where the colony of malignant cells grows. Growth of malignant cells in secondary sites disrupts organ function and increases the tumor burden on the host. Thus, there is a critical need to understand the factors regulating the spread of cancer cells to distant sites and their growth therein. Over half of all patients diagnosed with pancreatic ductal adenocarcinoma (PDAC) present with liver metastasis, and five-year survival for these patients is currently three percent. We performed an in vivo screen for PDAC metastasis suppressors using a human whole-genome shRNA library in order to understand factors regulating PDAC metastasis and identified Inter-α-Trypsin Inhibitor Heavy Chain 5 (ITIH5) as a suppressor of PDAC metastasis. Knockdown of ITIH5 significantly increased liver metastasis while high ITIH5 expression was correlated with rounded cell morphology and decreased cell motility and metastasis. ITIH5 is a secreted protein related to plasma protease inhibitors. To test the hypothesis that secretion of ITIH5 is required to suppress metastasis, we deleted the secretion signal sequence of ITIH5 (ITIH5Δs) and compared development of liver metastasis in highly metastatic PDAC cells expressing either control vector, secreted ITIH5, or secretion-deficient ITIH5Δs. Intriguingly, ITIH5Δs was sufficient to recapitulate the effects of secreted ITIH5 on cell morphology, motility and metastasis. These data suggest that ITIH5 may suppress metastasis by an intracellular mechanism not predicted by previously published reports. Understanding how intracellular ITIH5 attenuates PDAC metastasis could reveal new elements of PDAC biology that could become future therapeutic targets for patients affected by this aggressive cancer.

Acknowledgments

I would like to thank Drs. Chand Khanna, D.V.M., Ph.D., Michael Lizardo, Ph.D. and Arnulfo Mendoza, D.V.M. for their training in the Pulmonary Metastasis Assay (PuMA). They generously gave me hands-on experience with this challenging technique. Thanks to Kyle Strom, Ph.D., Joe Usset, Ph.D., Seth MacPherson, and John McGuire M.S. for their input on the automated image analysis project and especially to Ashley Tsue, whose tireless effort made the project possible. Thanks to Ken Sasaki, M.D. for his training in intrasplenic injections and to Sharon Manley, Ph.D. for her assistance with intrasplenic injections, extracellular vesicle isolation and for engaging scientific discussion. Thanks to Tomoo Iwakuma, M.D., Ph.D., Atul Ranjan, Ph.D. and Alejandro Parrales, Ph.D. for guidance, in molecular biology and gene expression experiments. Thanks to Evan Kauffman, Rosalyn Henn, and Aishwarya Parasuram Girija for their assistance with ITIH5 experiments. Thanks to Thomas Beadnell, Ph.D. and Adam Scheid, Ph.D. for engaging scientific conversations. Thanks to my wife, Elizabeth Young, M.S.N., R.N., C.N.E., for her long standing and comprehensive support without which, a career in science would not be possible. Thanks to the M.D., Ph.D. program at the University of Kansas Medical center for outstanding training, mentorship, fellowship and support. I would like to acknowledge and thank my committee for their effort in reading and editing my grant proposals, my thesis, guiding my projects, and for their support as mentors. I would like to thank my PI, Danny Welch, Ph.D. for the many opportunities he gave me to write, travel to conferences and for the privilege of doing science every day.

Table of Contents

List of Figures

List of Tables

Chapter 1 **- Introduction**

Biology of Metastasis

Cancer is a disease of intrinsic failed feedback inhibition: whereas normal cells respond to many homeostatic controls to keep the organism alive, cancer cells have lost this priority, grow unchecked and prioritize their own survival above all else. The spread of cancer cells to distant sites is called metastasis, which comes from the Greek word *methistanai,* which refers to a change in place, standing or position (*meta* "change"*, histanai* "to (cause to) stand, to place"). Metastasis is a particularly fearsome attribute of malignant cells because this spread can disrupt the function of otherwise uninvolved organs. Simultaneously, metastasis undermines the physician's ability to treat the cancer as a local disease and the patient's ability to regard it as such. Patients with metastatic cancer generally have a worse prognosis than patients with localized disease [1]. Thus, there is a critical need to understand metastasis so that therapeutic strategies can be developed to curb the spread of a patient's cancer and the toll the disease exacts from its host. Here, we will explore the biology of metastasis, tools for measuring this process and highlight pancreatic cancer as an example of how metastasis suppressors, genes that suppress metastasis without necessarily suppressing primary tumor growth [2], can be identified and studied to understand how they work to suppress metastasis in a cancer for which this spread occurs early, frequently and contributes to a poor patient prognosis.

While cancer may not obey the decreed guidelines for physiologic homeostasis, it is still constrained by the laws that govern all of biology such as the implications of thermodynamics for energy metabolism, membrane enclosed cells being the fundamental

system units, and selection on variation driving change in a population [3]. These constraints have implications for how cancer starts, evolves, spreads and is treated. Cancer appropriates processes from normal cell biology for its own survival. The cellular tools (e.g. proteins) used by cancer cells to perform a task like migration are the same tools used for migration in normal physiology. This then, may prove to be a double-edged sword—perhaps normal biology might be used as a platform for understanding the functions of these genes, transcripts and proteins co-opted by cancer for growth and metastasis. Next, we will explore the parallels between metastatic cancer cells and normal cells that use the same "tools", such as stem cells and so-called cancer stem cells. The goal is to draw out and understand themes that may be leveraged to understand the biology of metastasis and design rational future therapeutic strategies.

Parallels drawn between stem cells and cancer are not new [4] [i]. However, these shared features are becoming increasingly important as our understanding of disseminated, recurrent and metastatic cancer cell biology continues to develop. Indeed, nearly all cancer-related deaths are the result of recurrent and metastatic disease, highlighting the need for a more comprehensive schema of how tumors colonize new sites, resist therapy and evolve. In this chapter, we compare the phenotypes of stem cells, cancer stem cells (CSCs) and metastatic cells, highlighting notable points of contrast. We begin with an introduction to stem cell biology, tumor initiating CSCs, metastatic cells and discuss shared features. The implication of the stem-like phenotype extends to many

[i] The following four paragraphs previously appeared in Chapter 1 of Cancer Metastasis and Cancer Stem Cell/Niche, "Fundamental Relationships Between Cancer Stem Cells, the Cancer Stem Cell Niche and Metastasis." Pp. 3-23 (21), DOI: 10.2174/97816810834761160101. It has been updated here. See References [4].

characteristics of cell biology: cell division, differentiation, morphology, gene expression, motility, invasion, clonogenicity, capacity for colonization, metabolism and the interaction of these cells with their surrounding microenvironment. Stem cell phenotypes are highly complex and, while there may be a number of shared features, there are important elements that are uniquely tissue-dependent. While staunch definitions based upon a single biomarker of stemness have proven inadequate in broader applications, identifying universal themes of the stem cell phenotype may provide critical insights for studying cancer. Our understanding of this complex biology is critical for developing rational and dynamic therapeutic interventions for patients with recurrent and metastatic cancer.

The observation that features of a cancer cell resemble developmentally primitive cells dates back over 150 years [5]. This has proven to be a perspicacious observation indeed, given the similarities between cancer cells and stem cells with respect to their dynamic regulation of mitosis, gene expression, migration, metabolism and self-preservation. Cell division is a critical component of carcinogenesis and early observations prompted the notion that cancer may arise from a stem cell [6, 7]. Additionally, the therapeutic significance of cancer cells displaying a stem cell-like phenotype has been more recently appreciated after patients whose cancer was treated with chemotherapy and were without evidence of disease, experienced recurrence of disease months or years later. These observations suggested that there was perhaps a population of mitotically quiescent cancer cells unaffected by chemotherapy that survived, proliferated and gave rise to the recurrent tumor or metastatic disease [8]. Tumor-initiating cells are the proposed “cancer stem cells” (CSCs). Given the importance of these phenotypes in the control of cancer, here we compare the shared and distinct biological

features of normal stem cells, CSCs and metastatic cancer cells and consider the therapeutic significance of these insights.

Stem cells are populations of cells with the capacity to divide symmetrically, where the resulting daughter cells retain an equal potential to produce cells of a given lineage, or asymmetrically, resulting in more differentiated daughter cells that are narrowed in the variety of cells in that lineage they can produce [9]. It was thought that stem cells spend the majority of their cell cycle *in vivo* in mitotic quiescence [10], and upon stimulation by tissue damage or exogenous factors they can be induced to divide. More recently, in addition to quiescent stem cells, it has been shown that a population of Lgr5+stem cells also undergo active proliferation [11]. Daughter cells resulting from asymmetric divisions may become the more actively proliferating yet shorter-lived transit-amplifying cells which serve to regenerate tissue when required [12]. When stem cells are cultured *in vitro* however, conventional passaging methods may select for rapidly proliferating cells [13], explaining in part the dissonance between these two phenotypes. Ultimately, the orchestrated proliferation and differentiation of normal stem cells serve to reconstitute tissue lost to damage, aging and use. In a similar way, tumor cells remaining after selection by chemotherapy would be the “stem cells” of that tumor. These CSCs could eventually be stimulated to divide, resulting in the maintenance of slow-cycling CSCs. Stochastic changes in other daughter cells would re-establish tumor heterogeneity and a population of rapidly dividing cancer cells responsible for recurrence of disease.

Metastasis Suppressors

Metastatic cancer cells are defined by the ability to leave the primary tumor, enter and survive in the circulation, arrest at a different site and proliferate there to form a metastatic colony [14]. Enhancing any step along this cascade has the potential to increase metastatic efficacy, while a deficiency in any step will definitively avert metastasis. Metastasis is inefficient; less than one percent of the cells that enter the circulation are capable of forming a metastatic colony [15] and if disseminated cells are prevented from outgrowth after arriving at the secondary site, they will not form a metastatic colony [16].

As we have discussed above, cancer co-opts proto-oncogenes for survival, proliferation and migration to survive and spread. Conversely, tumor suppressor genes oppose cancer growth and spread. While tumor suppressors may slow both the growth of the primary tumor and metastasis, metastasis suppressors resist a cancer's ability to complete the metastatic cascade without necessarily affecting growth of the primary tumor [2]. Many metastasis suppressor genes have been identified and have been shown to suppress metastasis in multiple tumor types including melanoma [17], breast [18], colon [19], squamous cell carcinoma [20], prostate [21], ovarian [22], bladder [23] and pancreas [24]. These genes vary widely in their biochemical function and include kinases, integrin interacting proteins, chromatin remodeling complex components, neuropeptides, transcriptional coactivators and GTPase regulators. The goal of metastasis suppressor research is to understand the mechanism of metastasis suppression thoroughly enough to create a treatment that mimics the biological effect and effectively suppress human metastasis [25]. To date, this hope remains unrealized.

While their biochemical classifications are distinct, metastasis suppressors share a common ability to reduce metastasis when expressed. Suppression of metastasis may affect any step along the metastatic cascade. By observing the number, size and distribution of metastases, we may begin to gain insights into the suppressor's mechanism of action, that is, which step in the metastatic cascade it affects. The first metastasis suppressor gene to be identified was NM23 (also called NME1) in murine melanoma [26]. Its expression was significantly higher in poorly metastatic cells as compared to their highly metastatic counterparts. Other metastasis suppressors, like KISS1, reduce the size of the disseminated cancer colonies, suggesting an effect on disseminated cell proliferation at the secondary site [27]. Interestingly, while effects of KISS1 expression are minimal on the primary tumor, KISS1-expressing cells are dramatically suppressed in their ability to colonize multiple organ sites such as the lung, bone and kidney [28]. Another metastasis suppressor, Inter-Alpha-Trypsin-Inhibitor Heavy Chain 5 (ITIH5), seems to reduce both the size and number of metastases in addition to slight reductions in primary tumor growth, suggesting a more intrinsic effect on the cancer cells [29].

Quantification of Metastasis Assays

The quantification of metastasis is an important prerequisite for studying and understanding this complex process. Early efforts in studying metastasis recognized that while the natural history of metastasis involves spontaneous shed of cells from the primary tumor that seed a colony at a secondary site, experimentally seeding cancer cells into a secondary site by using an intravenous injection increased their ability to regulate

the variables of the experiment. In these early experimental metastasis assays, cancer cells were injected intravenously into a mouse to seed the first capillary bed they contacted, the lung. By using melanoma cells, the melanin produced resulted in black cancer cells that were easily visible on the surface of the lung at necropsy and aided in visual counting of gross metastases. An important observation regarding metastasis was made using these tools: metastatic efficacy is a phenotype that can be change under selective pressure, like most other processes in biology [30].

Methods for quantifying gross metastases in amelanotic cancers employed either a biological dye component in Bouin's fixative [31], India ink [32] or genetically labeled fluorescent reporters [33] to provide contrast against the lung tissue and to facilitate identification under fluorescent dissecting microscopes. All of these methods require euthanasia of the model animal however, and quantifying metastasis *in vivo* proved a more difficult problem. Luciferase reporters allowed for whole-body imaging of experimental animals bearing metastases [34] and provided quantification of tumor burden at the expense of resolution. The combination of fluorescent reporters to pre-existing methods for *in vivo* microscopy allowed for increased resolution of metastatic growth *in vivo* [35], which allowed for the study of cellular processes already known to be involved in metastatic colonization to be visualized in real-time. The development of *ex vivo* tissue culture techniques such as the Pulmonary Metastasis Assay [36] allowed for disseminated cancer cells to be grown in living tissue and for the study of factors affecting the growth of metastatic cells to be observed directly. Such methods of quantifying lung metastases are relevant to many different cancer types including both melanoma [37] and pancreatic cancer [38].

A remaining challenge in all of these methods is that the greater the biological relevance of a model (e.g. a genetic model that develops spontaneous metastases), the more challenging real-time imaging and quantification of those metastases becomes. Conversely, models best suited for high resolution imaging of the disseminated metastatic cells are often criticized for their lack of biological relevance. Models are generally tailored to answer a specific scientific question. Likewise, by definition, a model is intrinsically different from the process it is used to study as noted by the twentieth century statistician George Box, “All models are wrong, but some are useful” [39]. Thus it seems that the progression of models for the study of metastasis has been driven and will continue to be guided by the ability of the scientist to use the model to quantify elements of the metastatic process and the genetic, pharmacological and optical technologies driving such development.

Pancreatic Cancer and Metastasis

Pancreatic ductal adenocarcinoma (PDAC) is a deadly disease. It may have been described as early as the 18th century, [40] and has since been more thoroughly defined. It remains the fourth leading cause of cancer deaths for men and women [1] and unfortunately, a lack of effective treatment strategies is a persistent challenge in PDAC. This is illustrated by the fact that despite being the top four leading cause of cancer death, the incidence of PDAC does not rank within the top ten cancers diagnosed in men and is eighth on the list for women. This is in striking contrast to a disease like melanoma, where the incidence is high, ranking fifth in men and sixth in women, yet melanoma fails to number among the top ten list of cancers contributing to death. Melanoma primary tumors

are accessible to surgical excision, which is effective in reducing or preventing further morbidity and mortality to the patient [41]. Furthermore, recent advances in systemic therapies, such as immunotherapy, have proven effective in treating disseminated melanoma [42]. Patients diagnosed with PDAC do not have such therapeutic advantages, which is reflected in the current prognosis of this disease. The overall five-year survival for pancreatic cancer is only eight percent. Astoundingly, over half of all patients diagnosed with pancreatic cancer (52-56%) are diagnosed with disseminated disease. The liver is a common site for metastasis [43] and for these patients, the five-year survival is only three percent. Understanding the causes of PDAC tumorigenesis and metastasis are critical for the development of effective treatments for this devastating disease.

Pancreatic cancer is defined by a small number of driver mutations found in the vast majority of these tumors: KRAS, p53, p16 and SMAD4 [44]. These same mutations have inspired a number of mouse models of pancreatic cancer [45]. While it seems that a defined number of mutations define the progress of PDAC tumorigenesis, these same driver mutations are retained within the metastases and at present, there are no known analogous mutations acting specifically as drivers of metastatic spread of pancreatic cancer [46]. One question that arises then, is if genes are not being selected to drive metastatic progression, which other transmissible markers of cellular function are? Other possible cellular targets include epigenetic modifications to DNA and histones. Epigenetic marks such as methylation, acetylation, phosphorylation, ubiquitination and sumoylation affect gene expression and are both stable enough to be transmitted for selection [47] and have been shown to change during PDAC metastasis [48]. Thus, they represent a field ripe for the study of tumor evolution.

Epigenetic modifications stably affect gene expression without modification of the DNA sequence and are actively regulated during dynamic biological processes such as development [49]. Like development, the metastatic cascade requires dramatic changes in gene expression and cell behavior. In pancreatic cancer, there is accumulating evidence that such changes may indeed be critical for metastatic progression [46, 48, 50]. Understanding the changes required for metastasis and selected for during tumorigenesis are critical for understanding and curbing the spread of pancreatic cancer. Currently, two clinical trials aim to detect epigenetic changes in metastatic PDAC [51, 52], but neither attempt to therapeutically modulate chromatin regulation.

Inter-alpha-trypsin-inhibitor-heavy chain Family

In order to identify genes regulating PDAC metastasis to the liver, we performed a genome-wide screen in a non-metastatic human PDAC cell line, S2-028 [29]. This screen identified two suppressors of pancreatic cancer metastasis: HMP-19, which was validated as a suppressor of PDAC metastasis, and Inter-Alpha-Inhibitor-Heavy-Chain 5 (ITIH5). The inter-alpha-inhibitor family (IαI) are a family of secreted serine protease inhibitors that were discovered serendipitously in 1961 by the Loeb lab in Paris, France while attempting to isolate haptoglobin from the plasma [53]. Originally called protein π (pi), it was identified that these proteins were different from ceruloplasmin, haptoglobin and α_2-macroglobulin. IαI proteins contain three main functional domains: vault protein inter-alpha trypsin (VIT) domain, Von Willebrand factor type A (VWA) domain and an inter-alpha-trypsin inhibitor heavy chain (ITIH) domain, hereafter referred to as the multi-copper oxidase domain (MCOD) [54]. The fact that IαI were found by the Loeb group to not contain copper or

oxidative activity makes their MCOD domain a potential cause for confusion. However, the IαI MCOD domains are similar to the MCOD of ceruloplasmin, the major copper carrying protein in the body [55]. It is possible then IαI can indeed bind copper via this domain although this has not been definitively demonstrated for ITIH5.

The IαI have a complex structure and post-translational processing. They are composed of a light chain (Bikunin) and two heavy chains (IαI). The light chain is transcribed from the Alpha-1 Microglobulin/Bikunin Precursor (AMBP) gene on chromosome 9, while the heavy chains ITIH1, ITIH2, ITIH3, ITIH4, and ITIH5 are transcribed from the IαI genes on chromosomes 3, 10, 3, 3 and 10 respectively. Extracellularly, the light chain and the heavy chain are each proteolytically cleaved before being finally covalently linked to chondroitin sulfate or, in the case of the heavy (IαI) chains, binding hyaluronic acid (HA) present in the serum or extracellular matrix [56].

While IαI are structurally similar to serine protease inhibitors, the majority of the protease inhibition has been attributed to Bikunin, which in total, only accounts for approximately 5% of the protease inhibitory activity present in the serum [56]. In normal physiology, ITIH5 is the strongest expressed IαI in the placenta, skin, breast, adipose and pancreas [57]. Specifically, ITIH5 is expressed in the pancreatic islets and pancreatic ductal epithelium [29]. Interestingly, while ITIH1-4 are robustly expressed in the liver, ITIH5 is not, suggesting perhaps a different function compared to other members of this family. ITIH5 is the predominant IαI in the skin, and is expressed by dermal fibroblasts but not keratinocytes [58]. Its expression increases in inflammatory skin diseases such as psoriasis and ITIH5 knockout mice show extreme thinning of the epidermis, suggesting a role for ITIH5 in the maintenance of skin homeostasis.

A number of remaining questions surround the role of IαI and ITIH5 in normal physiology and in cancer. A tumor suppressive role has been attributed to ITIH5 in a number of cancer types including: breast [54, 59, 60], bladder [61], lung [62], tongue [63], central nervous system [64], acute myeloid leukemia [65], colon [60], stomach [66], pancreas [29] and thyroid [67]. It has been demonstrated that ITIH5 may change the epigenetic state and activation of Rho/Rac signaling [68] and gene expression [69], but as of yet, no definitive mechanism has been shown to fully explain its tumor suppressive activity.

Chapter 2 **- Comparative Biology of Metastasis and Development**

The Cancer Stem Cell Phenotype [ii]

Discussion of CSCs envelops many concepts related to the origin of malignant cells, how selective processes change the tumor cell population over time (i.e. tumor progression), the ability of cells to successfully colonize new sites (i.e. metastasis), and the features of therapy-resistant cancer cells in disease recurrence (summarized in Table 2-1 and Fig. 2-1). Although a so-called "tumor-initiating cell" may very well fit many of the aforementioned criteria, this nomenclature describes many of the later aspects of CSC biology without reference necessarily to their origin, with which we begin our discussion.

Morphologic observations of cancers and embryonic tissues gave rise to the first ideas connecting cancer with stem cells. The strikingly heterogeneous composition of teratomas, containing teeth, hair, and sundry embryonic tissues led to the hypothesis that these tumors may come from a stem cell [70, 71]. Further studies extended this observation and demonstrated the stemness of teratoma cells by showing their potential to differentiate into a multitude of tissues [72]. Beyond potency, normal stem cells, tumorigenic cancer cells and metastatic cells must all have the capacity for continued proliferation, from even a single cell [73]. However, it was observed in leukemia that many of the cancer cells had a finite ability to self-renew, which incited the search for the tumor-sustaining CSCs in this disease. Cell surface markers were used to define a subpopulation of human CD34+CD38- acute myeloid leukemia (AML) cells capable of

[ii] The following chapter previously appeared in Chapter 1 of Cancer Metastasis and Cancer Stem Cell/Niche, "Fundamental Relationships Between Cancer Stem Cells, the Cancer Stem Cell Niche and Metastasis." Pp. 3-23 (21), DOI: 10.2174/97816810834761160101. It has been updated here. See References [4].

recapitulating an AML phenotype in SCID mice [74]. This subpopulation was less differentiated than the other cells and provided evidence that a defined population of resident stem cells is responsible for AML.

Table 2-1: Similarities between Stem Cells, Cancer Stem Cells and Metastatic Cells[iii]

	Shared Features	Distinguishing Features
Mitotic Rate	Both slow and actively-cycling populations exist [10, 75].	Slow-cycling CSC populations are tumorigenic and can be chemotherapy resistant [76]. Actively-cycling CSC populations drive tumor progression [77].
Genomic Intregity	Normal stem cells maintain their genomic integrity.	CSCs[78] and metastatic cells [79] are genetically unstable.
Dormancy/Quiescence	Cells may remain dormant or be triggered to actively proliferate [10].	
Surface Markers	Common markers are shared in mammary cells [80] and HSCs [74].	Stem cell, CSC and metastatic cells markers are vary by tissue. Markers may also vary within a tissue [81-83].
EMT	Expression of EMT related markers can be observed [80, 84, 85].	Reversal of EMT (MET) related markers facilitates metastatic colonization [86, 87].
Self-Renewal	Must be able to self-sustain and reconstitute the tissue, even from a single clone [12, 74].	
Motility	Have the capacity to migrate from the original site and colonize a new site [88, 89].	Motility may or may not correlate with metastatic capacity [16, 89].
Invasiveness	Can invade or migrate through surrounding tissues [88, 90]	Invasiveness is necessary but not sufficient for metastasis [90, 91].
Metabolism	Generally show increased glycolytic activity [89, 92-94].	
Drug Resistance	Not inherently drug resistant, depends upon mitotic rate and phenotype.	Drug resistance does not guarantee metastatic potential.
Niche	Provides protection, support and regulates growth [95, 96].	Cancer associated niches do not suppress respective cells. Metastatic niches are continually remodeled [97].

[iii] While not exhaustive, this table highlights general trends and shared features between normal stem cells, cancer stem cells (CSCs) and metastatic cells.

Figure 2-1: Properties of Stem Cells, Cancer Stem Cells and Metastatic Cells

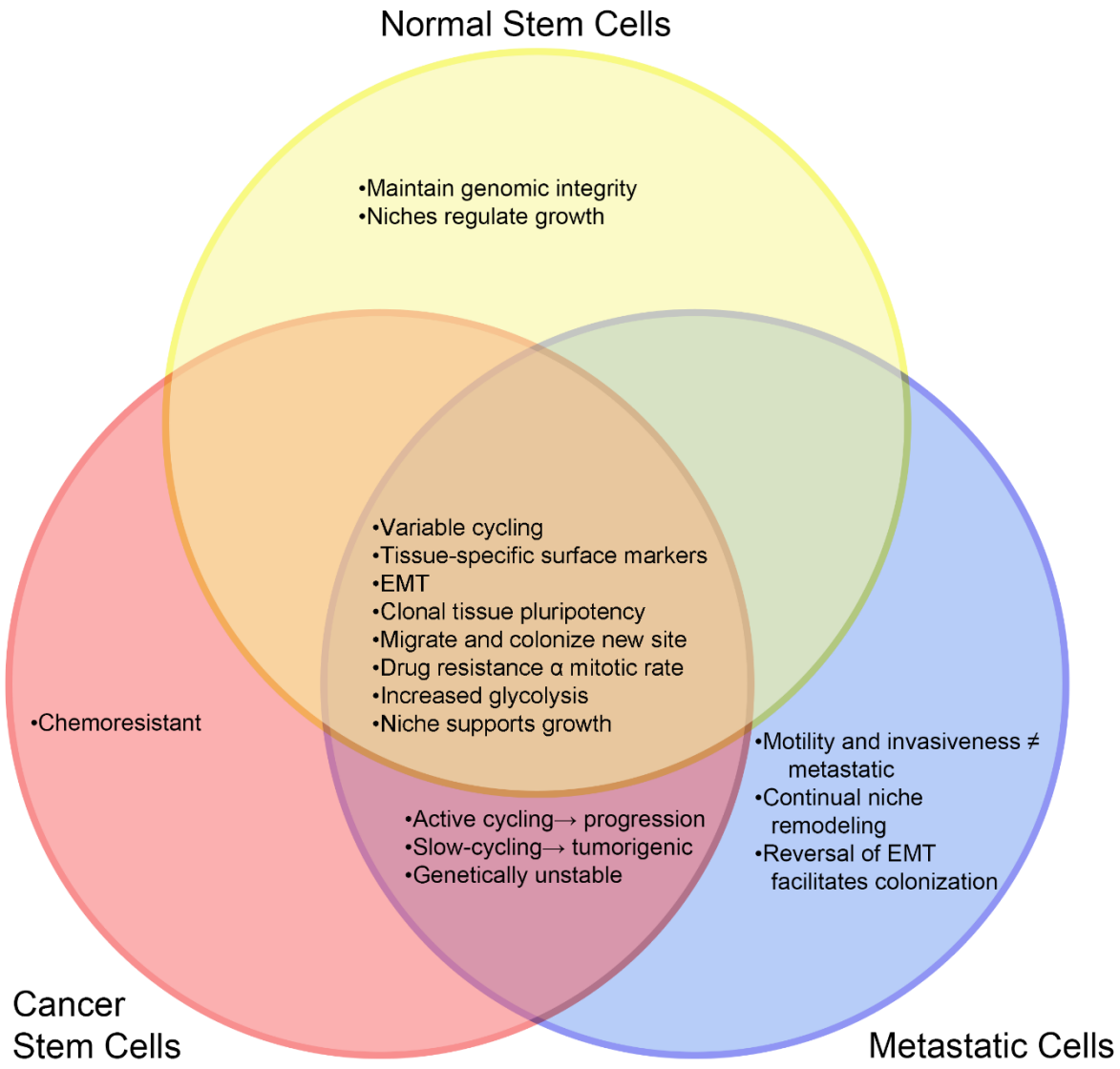

Mitotic Activity

There is also evidence for a relationship between the state of differentiation and tumorigenic capacity in squamous cell carcinomas, where it was demonstrated that poorly differentiated cells were the fastest cycling cells in the tumor [75]. As squamous cell carcinoma cancer cells differentiated they became less mitotically active and less

tumorigenic, suggesting that there was a primordial population of cells responsible for persistence of the tumor and that the cancer cells entered mitotic quiescence as they differentiated. The net mitotic index of malignant cancer cells is generally constitutively high, a feature that has been exploited by conventional chemotherapies for the past 75 years [98]. Stem cells in the hilum of the ovary have been demonstrated to be both slow-cycling and prone to tumorigenesis after tumor-suppressor loss [99], suggesting a role for these slow-cycling, normal stem cells in the development of ovarian carcinomas. CSCs are hypothesized to have a low mitotic rate that aids in rendering them resistant to traditional chemotherapeutics targeting rapidly proliferating cells. Supporting this hypothesis, a relatively slow-cycling population of CSCs was shown to drive tumor growth in glioblastoma [100]. In an intestinal adenoma model, it was demonstrated that Lgr5+ stem cells divide and contribute to tumorigenesis, although this cycling population was unable to reinitiate tumors [101]. These results emphasize that a cycling subset of CSCs contribute to tumor progression, although they may be intrinsically sensitive to treatments targeting rapidly proliferating cells. Slower-cycling CSCs are important in tumorigenesis and in driving recurrence of disease, especially in the context of a post-chemotherapeutic setting.

Protein and Biomarker Expression

While these data suggest that tumor-initiating cells have the capacity for continued proliferation and differentiation, the identity of CSCs in many solid tumors remains unclear. Solid tumors are a complex amalgamation of normal (endothelial cells, fibroblasts, immune cells, etc.) and neoplastic cells whose dynamic interaction may

positively [102, 103] or negatively regulate tumor progression [104] and metastasis [105]. In the absence of morphologic features to distinguish differentiated cancer cells from stem cells, biomarkers of these states are required. Identifying appropriate biomarkers and physically separating them from their surrounding microenvironment makes the lineage tracing and clonal passaging experiments required for definitive demonstration of CSC contributions in solid tumors challenging. It is expected that markers of solid tumor CSCs will be unique to their tissue of origin (i.e. markers of breast CSCs will differ from intestinal CSCs) just as markers of normal stem cells vary by tissue, there are not yet unified markers of solid tumor CSCs within a given tissue, although many candidates have been identified. This is illustrated by data from mammary tumors, where a population of cells defined by CD44+/CD24-low expression was shown to have an increased capacity for tumorigenesis [81]. Other groups have identified CD61/β3 integrin as biologically relevant markers used to identify mammary CSCs [106]. Stem cell antigen 1 (Sca1) has also been identified as a marker of mammary stem cells, which are also resistant to ionizing radiation [83]. This variation in mammary stem cell markers could be a consequence of technical variation or differences in the model systems. However, these data might also suggest that, in the mammary gland, the CSC phenotype may not be solely dependent upon a static, defined set of biomarkers. Instead, the tumorigenic and differentiating capacity of CSCs reflects a multitude of intrinsic and environmental factors. In this case, the expression of various biomarkers may be an effect and not a cause of more profound biological interactions. Indeed, in solid tumors a number of prospective biomarkers have been proposed [80, 81, 89, 106-108], but it is unlikely that a uniform set will concisely define CSC biology. As compared to carcinomas, tumors of neural crest origin have come

from cells whose role in normal physiology involves delaminating from an epithelia (epithelial to mesenchymal transition), migrating to a distant anatomical site, and colonizing it [109]—features shared with metastatic cells. Similarities between embryonic neural crest migration and metastasis of neural crest derived tumors are illustrated by the expression of genes such as Slug, which is expressed during both the migration of melanocyte precursors from the neural crest and in melanoma during metastasis [110]. Mechanisms by which normal stem cells from the neural crest migrate to and colonize new tissues may share common biologic means with metastatic cells which are required to complete similar tasks to survive and proliferate to colonize new tissues.

Metabolism

Altered cell metabolism is another shared feature between stem cells, CSCs and metastatic cells. The propensity of cancer cells to use primarily aerobic glycolysis as opposed to oxidative phosphorylation (OXPHOS) has been known for almost 90 years [111] and has been observed in stem cells more recently [112-114]. Ovarian cancer cells grown in spheroid culture consumed higher amounts of glucose than their counterparts cultured in 2D culture, demonstrated expression of stem-cell related genes and had increased tumorigenic capacity [89]. Melanoma cells whose metabolism was comprised primarily of aerobic glycolysis readily metastasized, whereas those whose metabolism had been shifted toward OXPHOS did not [115].

Importantly, while both stem cells and cancer cells have increased glycolytic activity as compared to most differentiated and mitotically quiescent cells in the body, differences between the two would permit the targeting of cancer cells, while preserving

normal stem cell function. An illuminating example can be found in hematopoietic malignancies. Hematopoietic stem cells (HSCs), hematopoietic progenitor cells and leukemia cells were all found to be sensitive to a reduction in lactate dehydrogenase (LDHA). However, the HSCs could tolerate reduced levels of the upstream glycolytic enzyme pyruvate kinase (M2 isoform), whereas the hematopoietic progenitor cells and leukemia cells could not [116]. The authors propose that this gap between the metabolic requirements of HSCs and leukemic cells offers a therapeutically tractable window. Together, these results show that normal stem cells, cancer stem cells, and metastatic cells all rely heavily upon glycolysis for cell metabolism. The exaggerated sensitivity of the cancer cells to changes in cell metabolism opens the possibility of targeting cancer cell metabolism to assess and/or treat neoplastic disease.

Metastasis Initiating Cells

What then are the factors that are required for successful metastatic outgrowth? Metastatic lesions are commonly associated with aggressive primary tumors with a high mitotic rate, although competition for resources within an actively proliferating tumor cannot solely explain the progression of metastatic disease. However, these trends are punctuated by numerous exceptions, concluding an imperfect relationship. For example, carcinoid tumors readily metastasize despite their generally indolent growth rates [117, 118]. In the skin, basal cell carcinomas, glioblastoma multiforme [14], and desmoid tumors [91] are readily invasive, yet rarely metastatic. Thus, an invasive tumor is not necessarily metastatic if these cells fail to colonize a new site.

Epithelial-to-Mesenchymal Transition

During development, cells leave the crest of the neural tube, migrate and become incorporated into tissues such as the facial bones, skin and gut. Their delamination from the neural tube, migration and accompanying phenotypic changes are known as the epithelial-to-mesenchymal transition (EMT). Similar changes are hypothesized to occur as epithelial cells from a carcinoma leave the primary tumor and migrate to a potential metastatic site. As the epithelial phenotype is also observed in metastatic cells, the reverse changes are thought to occur at the metastatic site, a process known as mesenchymal to epithelial transition (MET) [87]. Classically, the increased motility of cells having undergone EMT is facilitated by decrease in the cell adhesion protein E-cadherin and increases in the expression of the intermediate filament protein vimentin and the transcription factors Snail, Slug and Twist. Changes in similar gene expression patterns have been observed in metastasis [84], however to elicit changes in metastatic efficacy the functional consequences of these EMT-like changes must extend beyond facilitating cell delamination and migration.

Expression of the transcription factors Slug and Sox9 have been identified as markers of the basal and stem cells in the mammary epithelium [80]. Their expression increases the capacity of mammary epithelial cells to form organoids *in vitro* and reconstitute the mammary gland, suggesting that Slug and Sox9 are markers of the stem cells in the mammary epithelium. In addition, knockdown of Slug and Sox9 decreased formation of macroscopic metastases in an intravenous (IV) experimental metastasis model, correlating the stem cell phenotype with efficacy of metastatic colonization at the secondary site by disseminated cancer cells. During normal development, Sox9 functions

to sustain migrating cells from the neural crest on their journey to the peripheral tissues [46]. Although Slug and Sox9 have been detected in human breast cancers, they have not been identified as markers in metastatic breast tumors per se [80].

There exist other normal physiologic processes that mirror activities of metastatic tumor cells. Hematopoietic cells and immune cells migrate to a distant site and extravasate in response to chemokines. The C-X-C chemokine receptor type 4 (CXCR4) and C-X-C motif chemokine 12 (CXCL12 or stromal-derived factor 1/SDF-1) receptor-ligand relationship functions in normal physiology to attract lymphocytes to sites of inflammation [119] or to the bone marrow [120], and is also overexpressed in cancer cells that metastasize to the bone [121]. Thus, genes that facilitate metastasis may reflect a commandeering of normal developmental and immune programs. Interestingly, expression of CXCR4 has been shown to be upregulated by transformation-related protein 63 (TP63), conferring increased capacity for colony formation, anchorage-independent growth and chemotaxis [122]. These results suggest that there is overlap between the features of metastatic cancer cells and stem cells, despite the fact that these data do not demonstrate direct evidence for increased capacity of CXCR4 expressing cells to colonize the secondary site and complete the metastatic cascade. Thus, in many cases, metastatic cells are co-opting normal processes and mechanisms to facilitate progression of disease.

Mechanisms of Metastasis

Intriguingly, the induction of EMT results in expression not only of the expected mesenchymal proteins, but also of stem cell markers [123]. These mammary cells were

also more tumorigenic after having undergone EMT. Expression of Twist was shown to be required for metastasis of mammary carcinoma cells [124]. In pancreatic cancer, expression of Snail maintained expression of aldehyde dehydrogenase (ALDH), considered to be a marker of stem cells [92]. Hypoxia can induce EMT [125] and other pro-survival pathways. Subsequent up-regulation of HIF-1α and related target genes is a mechanism by which cells increase motility, invasiveness and their capacity to cope with increased amounts of unfolded proteins, serving to enhance metastasis [126]. However in colon cancer driven by L1, a neural cell adhesion molecule downstream of β-Catenin, changes in EMT related genes were not observed in cells overexpressing L1. These cells demonstrated increased motility, invasiveness and capacity for metastasis (L1-mediated colon cancer cell metastasis does not require changes in EMT and cancer stem cell markers). Others would suggest that the changes observed within EMT are within the plasticity of epithelial function, and that the changes observed do not necessarily provide evidence for differences in cell identity [127]. These results suggest that metastasis and the factors facilitating metastatic colonization do not necessarily require EMT, although EMT-like changes in gene expression are one means by which to arrive at the same biological end.

Disseminated cancer cells must arrest, survive and proliferate at the secondary site to form a metastatic colony. Interestingly, suppression of EMT related genes appear to indeed be one component of successful colonization. Loss of the homeobox gene Prrx1 both abolished the EMT phenotype and was shown to be required for successful metastatic colonization [86]. An epigenetic regulator of homeobox genes, Bmi-1, was

shown to direct self-renewal in mammary cells [128] and has also been shown to be required for tumorigenesis in colon cancer [129].

However, overexpression of the homeobox gene Goosecoid was found to increase both the motility of breast cancer cells *in vitro* and the number of metastases in an experimental metastasis model [130]. The observation that both overexpression of homeobox genes (Goosecoid) and suppression of homeobox genes (Prrx1) result in increased metastasis suggest that there remains much to be understood about the temporal and spatial regulation of EMT-related genes with respect to their influence on metastatic efficacy. Doublecortin-like kinase 1 DCLK1, found in circulating CSCs [85] and overexpressed in renal cell carcinoma, was found to regulate EMT in these cells and to have a distinct pattern of promoter methylation [131]. These data suggest that epigenetic regulation may be a common mechanism regulating the activity of normal stem cells, CSCs and metastatic cells that govern cell decisions regarding renewal and differentiation.

Contributions of the Niche

The architecture of the normal stem cell niche is tissue dependent, but in all cases it refers to the three-dimensional space surrounding normal stem cells that provides the stem cells with physical protection, nutrients and signals that direct stem cell behavior [95]. Indeed, one of the functions of the stem cell niche is to regulate the proliferation of stem cells to ensure that these cells with such profound proliferative capacity do not divide continuously [132]. Thus, the absence of the stem cell niche *in vitro* to suppress unnecessary proliferation also helps to explain the brisk mitotic phenotype observed

there, in addition to any added effect the process of conventional cell culture may contribute toward selecting for rapidly dividing cells.

The niche supporting CSCs by definition then differs in this regard [133], as proliferating cancer cells have already overridden growth inhibitory signals. Like the niche of the normal stem cell, the CSC niche provides the requisite protection and nutrients for CSCs [96] and indeed may use the same signaling molecules to influence the mitotic activity of CSCs [134]. The importance of maintaining dormancy is also highlighted in the context of metastasis. Progression of metastatic disease may occur months to years after anticancer therapy, suggesting that disseminated cells existed in a dormant niche or state. What are the stimuli that induce this awakening from dormancy and what are the signals that would maintain it? Notch signaling was shown to regulate the proliferation and capacity for sphere formation of tumor cells in glioblastoma multiforme (GBM) [135]. The authors conclude from these data that Notch signaling promotes the CSC phenotype in GBM, although an alternative explanation might be that the GBM cells are dependent upon the endothelial cells and that the decrease in GBM CSC is an effect of a decrease in endothelial cell number.

By comparison, the metastatic niche refers to the immediate microenvironment surrounding disseminated and seeded, potentially metastatic cells and it also helps to facilitate cancer cell growth. The secondary site where disseminated cancer cells will eventually invade and proliferate as a metastatic colony is termed premetastatic niche before the arrival of the tumor cells [136]. Interestingly, the pre-metastatic niche has been shown to be “primed” by HSCs from the bone marrow prior to colonization by disseminated tumor cells [137]. This action is initiated by factors released from the

primary tumor and results in upregulation of fibronectin in the niche fibroblasts and increased retention and growth of metastatic cells at the secondary site. Interestingly, the features of the normal stem cell niche may also provide necessary interactions to foster the growth of metastatic cells to those sites. For example, breast cancer cells metastatic to the bone received growth signals initiated by heterotypic cadherin interactions between the metastatic cells and the cells forming the osteoblastic and HSC niche [138]. The metastatic niche not only supports the growth of metastatic cancer cells, but is also dynamically regulated as the cells colonize the secondary site. Exosomes are one means by which this remodeling of the metastatic niche is mediated [139].

Conclusion

In conclusion, normal stem cells, CSCs and metastatic cells share many features including the ability to migrate [88, 110], synergistically interact with the surrounding microenvironment or niche for growth signals [102, 132, 137], resist apoptosis [9] and recapitulate from clonal origins the heterogeneity observed within the original tumor or tissue [74, 80]. The ability to successfully adapt to a changing environment is a necessary and shared feature of normal stem cells, CSCs and metastatic cells. Migratory stem cells of the neural crest and metastatic cancer cells must adapt to the physical environment at new locations while CSCs must adapt to changes in the local environment due to selective pressures present within a tumor (e.g. competition for nutrients or oxygen, anti-cancer therapy, etc.). One means by which this phenotypic plasticity is accomplished both during development and in cancer progression is by epigenetic regulation of gene expression. Dysregulation of the epigenome has already become a therapeutic target for cancer [140].

Requirements of a CSC include the ability to self-renew and proliferate indefinitely, to differentiate into cancer cells with more limited replicative potential and to be capable of reconstituting a tumor upon transfer. In essence, the fulfillment of Koch's postulates for CSCs of each tumor type will definitively establish the identity of the CSCs in various tumor types. However, isolation and serial passaging experiments required to definitively identify and study ostensible CSCs remain technically challenging, especially in solid tumors. For this reason, data that provide evidence for CSC contribution in different tumors vary greatly. As the identity of both CSCs and metastatic initiating cells continues to be elucidated, future therapeutic interventions must not rely upon a single biomarker for targeting and tumor destruction. Rather, a multi-faceted approach utilizing multiple, concurrent therapeutic interventions addressing different aspects of CSC biology is likely to be required for eradication of tumorigenic cancer cells. The reverse may also be true, as discoveries concerning CSCs and metastatic cells may also serve as a model for understanding the biology and regulation of normal stem cells, with important human applications for regenerative medicine. These considerations highlight significant

remaining questions Table 2-2 regarding the *in vivo* biology of cancer sustaining cells and implications for treating patients with cancer.

As our understanding of the biology and the selective process that produces the CSCs and metastatic cells expands, we may begin to therapeutically intercede on multiple fronts. What matters most to patients in distinguishing normal stem cells, CSCs and metastatic cancer cells is the identification of therapeutically targetable features. Ultimately, the relevance of our understanding this biology will be determined by the degree to which improved treatments produce better outcomes for patients with recurrent, disseminated and metastatic cancer.

Table 2-2: Remaining Unanswered Questions

- What is the *in vivo* mitotic rate of cancer stem cells and metastatic cells?
- What triggers the awakening from dormancy of cancer stem cells that causes recurrence?
- What makes CSC and metastatic cancer cells genetically unstable?
- Why is the genetic instability from CSCs and metastatic cancer cells not self-limiting?
- What therapeutically targetable featuresdistinguish CSCs from normal resident stem cells and other cells within the tumor?
- What traceable biomarkers can be used to detect CSCs?
- How will knowledge of CSCs direct patient treatment and follow-up?

Chapter 3 **– Quantitative Image Analysis Reveals Requirements for Metastasis Suppression by KISS1**

Introduction[iv]

Imaging plays a critical role in assessing components of living systems and understanding their biology as a whole. Qualitative imaging data are striking and give insight into biologic function, but quantitative analysis of imaging data remains challenging. Large variations in signal intensity, shape, or distribution can complicate objective and quantitative image analysis [142]. Such complex variations are often present within living systems and increase with the range of imaging depth [143]. While methods such as confocal microscopy allow for the independent imaging of each focal plane for subsequent data compilation, data collected using standard epifluorescence microscopy, *in vivo* imaging and time-lapse microscopy often capture images containing regions that are both in- and out-of-focus. Thus, out-of-focus objects within an image or light scattered as it is transmitted through tissues can skew quantification efforts [144, 145]. In metastasis research, image data from intact lungs, epifluorescence photomicrographs, *in vivo* luciferase, and Pulmonary Metastasis Assays (PuMA) [146] data all present such challenges. In these cases, objectively distinguishing between in-focus and out-of-focus fluorescent particles within the same image remains challenging.

PuMA is a powerful tool to study mechanisms of pulmonary metastasis *ex vivo* [147]. However, we found manual quantification of fluorescent image data to be time consuming and potentially subjective. In order to overcome these challenges, we

[iv] The following chapter previously appeared in Clinical & Experimental Metastasis, February 2018, Volume 35, Issue 1-2, p. 77-86. It has been updated here. See References [141].

designed an automated workflow to identify images suitable for automated analysis and quantify in-focus regions of interest (ROI) by adapting a method originally developed to study sediment deposition [148]. The goal of this workflow is not to replace one method of microscopy with another (i.e. confocal with epifluorescence), as we recognize each imaging platform has unique strengths and limitations. Instead, we sought to improve the objectivity and speed with which complex datasets containing images and features of varying quantity and quality can be stratified and analyzed.

We developed this tool to measure the growth of cancer cells disseminated to the lung in order to use the PuMA as a platform to further dissect how the metastasis suppressor KISS1 suppresses melanoma lung metastasis [17]. We hypothesized that melanoma cells expressing KISS1 would be growth suppressed (i.e., dormant) in the PuMA, just as they appear *in vivo* [149]. Surprisingly, we did not see any difference in the rate of growth in the PuMA as measured by area of GFP positive cells in each lung slice. Nonetheless, these experiments were useful in developing a tool for automated quantification of PuMA and other imaging datasets containing images and data varying in quality and intensity.

Methods

Pulmonary Metastasis Assay

All animal studies were conducted in accordance with the Guide for the Care and Use of Laboratory Animals (National Institutes of Health). Protocol (#2014-2208) was approved by University of Kansas Medical Center Institutional Animal Care and Use Committee. The PuMA was performed as described [146] with modifications. Female

nude mice aged 6-8 weeks were intravenously injected with 50,000 enhanced green fluorescent protein- (GFP) expressing C8161.9 cells (human amelanotic melanoma, clone 9) [150, 151] suspended in 200 µl of 0-4°C Hanks Buffered Salt Solution (HBSS, Life Technologies, #14175-103). Cells circulated for 20 minutes and lodged in lung capillaries. Mice were euthanized using CO_2 before lungs were insufflated with a 1:1 mixture of media and agarose using an 18-gauge (GA) needle and 10 ml syringe. After tying off the trachea with suture, lungs were extracted and placed in sterile phosphate buffered saline (PBS) on ice. Lungs were cut into ~0.5-1 mm sections using sterile forceps and microdissection scissors. Sections were placed on media-saturated Gelfoam® (Pfizer-Pharmacia & Upjohn Co., #09-0315-08) in a 6-well cell culture plate for incubation and imaging. Media was replaced every 2 days.

Experimental Metastasis Assay

In order to seed the lungs with disseminated melanoma cells, injections were performed as previously described [27]. Briefly, 50,000 C8161.9 cells were suspended in 0-4°C PBS and injected into the tail vein in a volume of 100µl using a 27GA needle and 1mL syringe. Cells were allowed to grow *in vivo* for 5 weeks or until the animal was moribund. After CO_2 induced euthanasia, lungs were imaged grossly using a fluorescent dissecting microscope and tumor and lung tissues were collected for analysis. Macroscopic metastases were quantified by using the multi-point tool in ImageJ to count each metastasis visible on the surface of the lung.

Cell lines and cell culture

Human PDAC cell lines (C8161.9) were cultured in DMEM/F12 with 5% fetal bovine serum (FBS, Atlanta Biologicals, # S11195), 1% glutamine (Gibco, # 25030-081) and 0.25% non-essential amino acids (NEAA, Gibco, #11140-050) in a humidified incubator at 37°C.

Immunoblotting

Conditioned media was collected from PuMA experiments and spun at 1,000rpm to pellet cellular debris. Media was mixed with loading dye and ran on a 10% acrylamide gel, transferred to a PVDF membrane and blocked with 5% nonfat milk in Tris buffered saline with Tween-20 (TBST). Primary antibody against KISS1 (custom mouse) was applied 1:1000 in block and allowed to incubate overnight before applying the anti-mouse HRP conjugated secondary (GE #NA931) for 1hr at room temperature.

Image Acquisition

Lung sections containing disseminated GFP-expressing melanoma cells were imaged at days 0, 7, 14 and 21. Each Gelfoam® sponge containing lung sections and cancer cells were placed lung side down on a culture dish (MatTek, #P35-G-1.5-20-C) for imaging. A Nikon Eclipse TS100 Inverted Microscope, QImaging QIClick monochrome CCD camera and Metamorph software were used to take ~30 non-redundant images per experimental group at 20x magnification for each time point (Figure 3-1a).

Figure 3-1: PuMA Image Acquisition and Automated Image Analysis Workflow

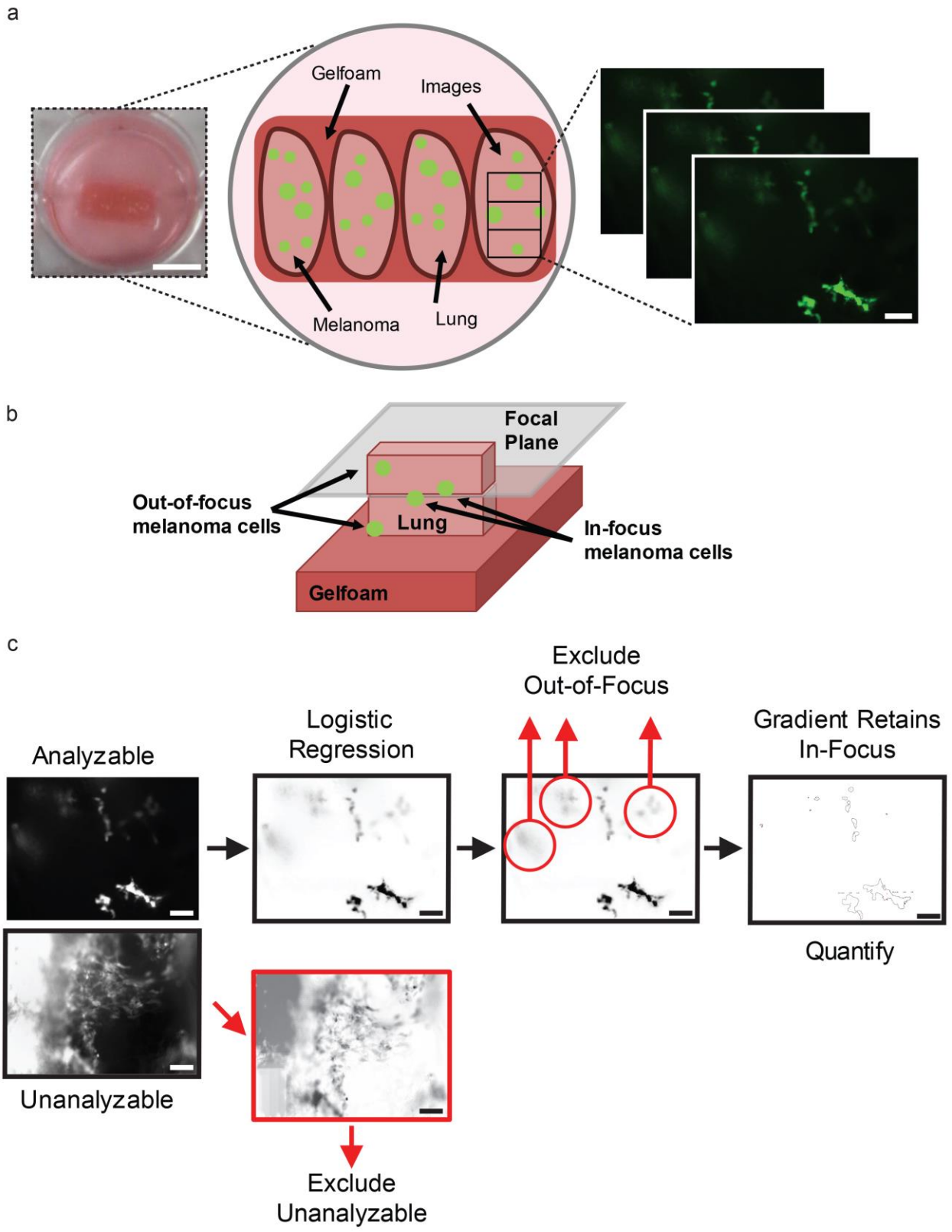

Figure 3-1 PuMA image acquisition and automated image analysis workflow. (a) Mouse lung sections (0.5-1mm thick) containing disseminated GFP-expressing melanoma cells were placed on media-saturated gelfoam sponges cultured ex vivo for up to three weeks. Using an inverted microscope, an average of 30 non-redundant photomicrographs were recorded per experimental group every seven days. Scale bar for cell culture dish is 1 cm. Scale bar for fluorescent image is 50 μm. (b) Cross-section views of lung sections containing GFP-expressing melanoma cells within lung section atop Gelfoam® with respect to the focal plane of the image. (c) Schematic of the automated workflow used for image analysis. Output from a logistic regression model selects analyzable images for subsequent automated analysis. To standardize measurement of melanoma growth, only in-focus fluorescent cell clusters/regions of interest (ROI) were quantified. In-focus ROI were selected by applying a Gaussian gradient and selecting ROI with a clarity value above the in-focus threshold for quantification. Scale bars are 50μm.

GFP-expressing cancer cells were present throughout the lung section. The focal plane that optimized the number of in-focus cancer cells was chosen for each image. Immunofluorescence (IF) images were collected using a Nikon Eclipse 80i microscope, QImaging QIClick 8 bit monochrome camera and an XCite120PC light source. Five images per time point were collected and quantified using ImageJ. After imaging, gelfoam with lung sections was returned to the 6 well dish and media was replaced.

Image Analysis

In collecting and analyzing PuMA data, we noted that while some images were easily analyzed by automated processing, images with high background skewed analysis because the software was not able to recognize all GFP-expressing cells or groups of cells. Hereafter, these cell clusters will be referred to as regions of interest (ROI) (Fig. 3-2a). A step-by-step protocol for the method described (Supplementary 1) and all operating scripts required for the protocol are freely available online (https://drive.google.com/drive/folders/1zmjp_VW_Pnw7BdyeAut36DS1J6AoJ-QG?usp=sharing). To develop a training set for machine learning, we used a large set of images and manually stratified analyzable images by how accurately the automated threshold identified ROI. ImageJ [152] was used for image processing and cell

measurements. R was used for statistical analysis, and MATLAB was used to identify out-of-focus particles.

To process the images, first the MaxEntropy threshold [153] from ImageJ was applied to images from the PuMA. Then, we manually classified images into two groups: those that the MaxEntropy threshold accurately identified the fluorescent cells (“analyzable”) and those that were not (“unanalyzable”). In both the analyzable and unanalyzable image sets, parameters from ImageJ served as explanatory variables (numROI, avgArea, avgPerim, avgWidth, avgHeight, avgMajor, avgMinor, avgAngle, avgCirc, avgFeret, avgIntDen, avgMinFeret, avgAr, avgRound, avgSolidity). Parameter descriptions are provided in Table 3-1 and Supplemental Fig. 3-4a.

Next, we used these explanatory variables to fit a multivariate logistic regression against the outcome variable of whether an image was analyzable or unanalyzable. Features which contributed significantly to distinguishing analyzable and unanalyzable images were used to stratify future image datasets (Table 3-1). Examples of analyzable and unanalyzable images identified by the model are shown in Fig. 3-2b.

Figure 3-2: Validation of Image Analysis to Measure Tumor Cell Growth

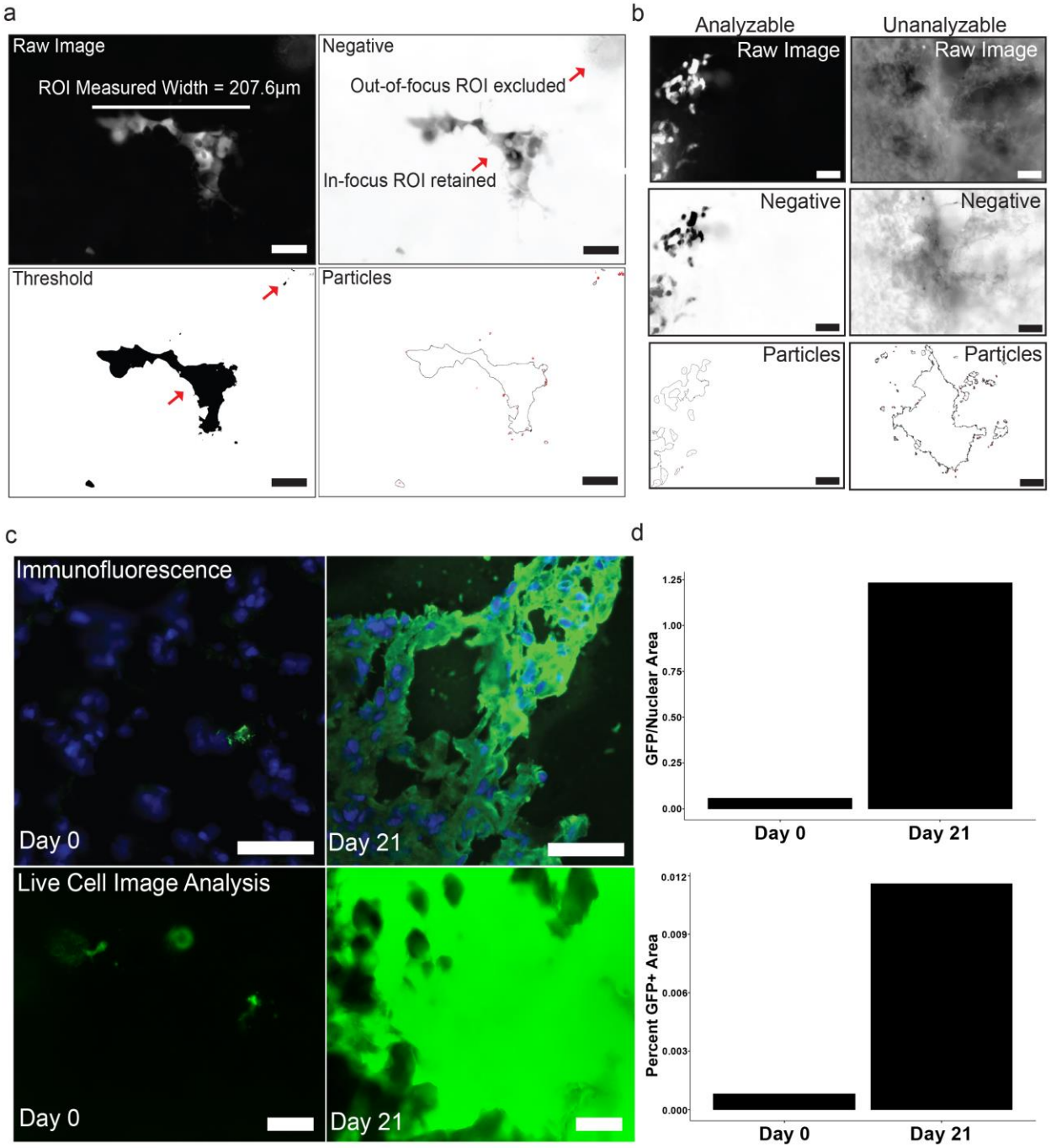

Figure 3-2 Validation of image analysis measurements and image stratification. (a) Image of disseminated GFP-expressing melanoma cells in living lung tissue. Raw image (monochrome), image negative, image after thresholding, and cancer cell(s) identified by ImageJ are shown. In-focus cell clusters/ROI are retained while out-of-focus particles are excluded. Width of cell cluster measured by ImageJ is scaled correctly. Scale bar is 50 µm. (b) Comparison of representative analyzable and unanalyzable images stratified by the logistic regression model. Raw images, negatives and ROI identified after applying the Gaussian gradient to identify in-focus ROI are shown. Analyzable images show correctly identified ROI, while unanalyzable images do not. Scale bars are 50µm. (c) Microscopy images of GFP+ control cells on Day 0 and Day 21 as seen by IF (upper panels) staining for GFP or live cell inverted epifluorescence microscopy (lower panels). Scale bars are 20µm (IF) and 50µm (image analysis). (d)

Quantification of tumor cell growth in the PuMA at Day 0 and Day 21 as measured by IF (upper graph) and image analysis (lower graph). Comparison of image analysis quantification with immunofluorescence (IF) show similar growth trends.

Table 3-1: Logistic Regression Identifies Features Predicting Analyzable Images

ROI Feature (Coefficients)	Definition	Estimate	Std. Error	z value	Pr (>|z|)
Width	Longest continuous horizontal dimension	88.840	19.330	4.596	4.300E-06 ***
Feret's Diameter	Longest distance between any two points	-94.700	21.980	-4.308	1.650E-05 ***
Height	Longest continuous vertical dimension	80.550	21.470	3.752	1.760E-04 ***
Aspect Ratio	$\frac{\text{Major Axis}}{\text{Minor Axis}}$	-15.360	4.462	-3.442	0.001 ***
Perimeter	Length of outside boundary	-12.860	4.587	-2.803	0.005 **
Solidity	$\frac{\text{Area}}{\text{Convex Area}}$	3.296	1.397	2.359	0.018 *
Roundness	$4 \text{ x } \frac{\text{Area}}{\pi \text{ x } [\text{Major Axis}]^2}$	-3.214	1.421	-2.261	0.024 *
Circularity	$4\pi \text{ x } \frac{\text{Area}}{[\text{Perimeter}]^2}$	-3.444	1.920	-1.793	0.073 ^
Minimum Feret	Minimum caliper diameter	-30.460	23.140	-1.316	0.188
Area	Area of the selection in square pixels	2.454E+09	1.883E+09	1.303	0.193
Minor Ellipse	Secondary axis of best fitting ellipse	-19.260	15.580	-1.236	0.216
Angle	Angle between primary axis and line parallel to the X-axis of the image	0.929	0.935	0.993	0.321
Major Ellipse	Primary axis of best fitting ellipse	7.788	16.200	0.481	0.631
Feret Angle	The angle (0-180 degrees) of the longest distance between any two points along the selection boundary (Feret's Diameter)	0.445	1.103	0.403	0.687

Table 3-1 Output of multivariable logistic regression. For each region of interest (ROI) feature assessed, the estimate, standard error, z value, probability that a value would be greater than the z value, and assigned significance codes are shown. Description of coefficients adapted from ImageJ User Guide imagej.nih.gov/ij/docs/guide/user-guide.pdf. Significance codes: 0 '***', 0.001 '**', 0.01 '*', 0.05 '^', 0.1 ' ', 1.

The outcome of our logistic regression was used to set a threshold for classifying which images were analyzable. To determine this threshold and assess prediction performance, we conducted a cross-validation using our test dataset by comparing original estimates of image analyzability from the multivariate analysis to the cross-validated model (Supplemental Fig. 3-4b). The probability threshold was set by constructing a 2x2 table comparing images determined to be analyzable by manual or automated stratification and determining which image probability value (0.57) gave the fewest misclassified images. Images with a predicted probability below this threshold were excluded from further analysis, while images with a probability above it were retained for further analysis. Comparison of automated and manual image stratification is summarized in Table 3-2. Overall, automated stratification performed well as a test for whether or not an image was analyzable with positive and negative predictive values of 0.957 and 0.678 respectively.

Table 3-2: Accuracy of Image Classification by Logistic Regression

		Manual Stratification (Truth)		
		Analyzable	Unanalyzable	Total
Automated Stratification (Test)	Analyzable	True Positives 1586	False Negatives 72	1658
	Unanalyzable	False negatives 156	True Negatives 328	484
	Total	1742	400	2142

Table 3-2 Comparison of manual and automated image stratification.

Finally, we selected only in-focus ROI for analysis using a method originally developed to remove out-of-focus ROI from images in sediment deposition research [148]. First, a clarity value is calculated for each ROI by applying a Gaussian gradient smoothing function. The threshold for in-focus ROI was determined by comparing a series of gradient-produced images with the original image. A clarity value threshold was set which distinguished between in-focus and out-of-focus ROI (Fig. 3-1b, 3-1c, 3-2a, 3-2b). ROI with a sharper gradient (larger value) than the clarity value were retained and the area was quantified, while ROI with a more gradual (smaller) gradient than the clarity value were considered out-of-focus and excluded. To verify our image analysis measured cell growth accurately, we compared image analysis measurements to direct measurements of cell growth using IF of GFP positive cells at Day 0 and 21 (Fig. 3-2c, 3-2d). We observed similar growth trends using these techniques, validating the measurements made by image analysis. Thus, we standardized the ROI which were

selected before calculating the surface area of the ROI. Surface area of the in-focus fluorescent ROI as compared to the total area imaged was then used as a proxy for cell growth *ex vivo* and we were able to automate the measurement of the tumor explants in living lung.

Statistical analysis

Logistic regression, one-way ANOVA, Student's t-tests and graphing were performed using R (Vienna, Austria) [154] and MATLAB [155].

Results

Our goal was to develop an automated workflow whereby epifluorescence images could be objectively quantified (Fig. 3-1a). Three tasks had to be automated in order to achieve this objective: (1) classification of an image as "analyzable" or "unanalyzable"; (2) measurement of ROI/cancer cell features in the image; and, (3) removal of identified out-of-focus ROI that might bias the data.

First, images were classified as "analyzable" or "unanalyzable". We found that some images were amenable to automated cell measurement (task 2) while some were not (Fig. 3-1c). All images unable to be measured must be removed from the analysis to avoid biased ensemble results (Fig. 3-2b). From our test dataset, we used several features measured by ImageJ (Table 3-1, Supplemental Fig. 3-1a) to stratify analyzable from unanalyzable images (Fig. 3-2b). Features varied in their ability to identify analyzable images and we found that ROI Width, Feret's Diameter, Height and Aspect Ratio were most significant in distinguishing analyzable from unanalyzable images (Pr (>|z|) of

4.300E-06, 1.650E-05, 1.760E-04, and 0.001 respectively). Also statistically significant were the ROI perimeter, solidity, and roundness (Pr (>|z|) of 0.005, 0.018, and 0.024 respectively). These features are a result of the statistical model built around our test data set and we would expect these features may vary for different data sets.

Table 3-3: Image Selection is Equitable Between Groups and Experimental Day

Day	Group Comparison	95% Confidence Interval (LL, UL)	*P* value
0	B-A	-3.189, 1.522	0.637
0	C-A	-2.689, 2.022	0.929
0	C-B	-1.855, 2.855	0.847
7	B-A	-7.080, 10.080	0.893
7	C-A	-10.080, 7.080	0.893
7	C-B	-11.580, 5.580	0.644
14	B-A	-9.010, 8.344	0.995
14	C-A	-8.844, 8.510	0.999
14	C-B	-8.510, 8.844	0.999
21	B-A	-9.562, 6.562	0.880
21	C-A	-5.729, 10.395	0.737
21	C-B	-4.229, 11.895	0.452

Table 3-3 Comparison of number of excluded images between biological groups. No difference was identified in the number of images excluded between any groups at any experimental day was identified after one-way ANOVA and Tukey's HSD post-hoc test.

Recognizing that several of the above referenced features may be potentially correlated (e.g. perimeter and area), we performed a cross-validation of our test set to check for over-fitting of our model and found that our model performed equally well on unique subsets of our data (Supplemental Fig. 3-1a). Next, we determined which

probability threshold would result in the fewest misclassified images and found this value to be 0.57. This threshold was then used to distinguish analyzable and unanalyzable images in future experiments. Common causes of unanalyzable images included decreased image contrast due to absence of fluorescent cancer cells, pixel oversaturation due to robust cancer cell growth, cancer cells outside the focal plane, and increased tissue density surrounding bronchioles producing increased background. We also compared the automated analysis to manual stratification (Table 2) and found that automated stratification was able to identify similar numbers of analyzable images as when the same dataset was analyzed manually.

Next, we wanted to ensure that there was not bias in our model between any of the biologically distinct groups analyzed. Over the course of a three-week PuMA experiment, lung sections from three biologically distinct lines of GFP-expressing C8161 melanoma cells were imaged at 0, 7, 14 and 21 days. Approximately 30 images (range, 14-58) were taken per experimental group at each time with a median and average of 25.5 and 29.8 images respectively (standard deviation, 10.9). To demonstrate that analyzable and unanalyzable images were stratified in an unbiased manner from distinct biological groups, we recorded the number of excluded unanalyzable images at each day of analysis and compared the means using one-way ANOVA and Tukey's *post hoc* test (Supplemental Fig. 3-1c). No statically-significant differences were identified between any of the groups. These data suggest that the image stratification is functioning equitably between biologic groups.

The second task was the measurement of the ROI features. The key steps involved in this process were: (i) removing broad-scale trends in the grayscale color of

the image; (ii) creating a binary image of black and white pixels through thresholding; and (iii) applying particle measurement routines to obtain quantitative data on the cell population (e.g., area, perimeter, long and short axis length and the orientation of long axis) for each ROI. Similarity between the ROI observed in the raw image and the ROI particles identified by the set thresholds (Fig. 3-2a, 3-2b) suggests that the threshold is able to correctly identify ROI of interest.

The third and final step was to exclude from further analysis any ROI that were out-of-focus and might bias the data. In this way, we could objectively select high quality images and quantify the area of in-focus ROI to standardize analysis between samples.

This workflow was developed while we attempted to elucidate the mechanism of KISS1 suppression. While the ability of KISS1 to strongly suppress metastasis [17] has been demonstrated in multiple tumor types [149] and there have been hints related to upstream and downstream regulatory pathways [156], the biochemical underpinnings of KISS1 metastasis suppression remain largely unknown. However, previous studies showed that KISS1 allows all steps prior to colonization of secondary sites [28]. As a result, we sought to use the PuMA as a model for understanding KISS1 mediated suppression in the lung so that we could test what regulates KISS1's metastasis-suppressing activity.

To our surprise, there was no statistical difference in the growth of KISS1-expressing cells compared to controls (Fig. 3-3a). In some cases, growth in lung appeared even greater (Fig. 3-3b). Since secretion of KISS1 is required to suppress metastasis [28], we confirmed that KISS1 was still secreted in the PuMA at Day 21 by immunoblot (Fig. 3-3c). Together, these data show that the outgrowth of KISS1-

expressing cells is not due to loss of KISS1 expression. In parallel studies using a classical *in vivo* model, the same KISS1-expressing C8161 cells were still robustly suppressed for metastasis despite seeding lung *in vivo* (Fig. 3-3d, 3-3e).

Figure 3-3: KISS1 Expression Does Not Suppresses Growth in the PuMA, but Suppresses Robustly in vivo

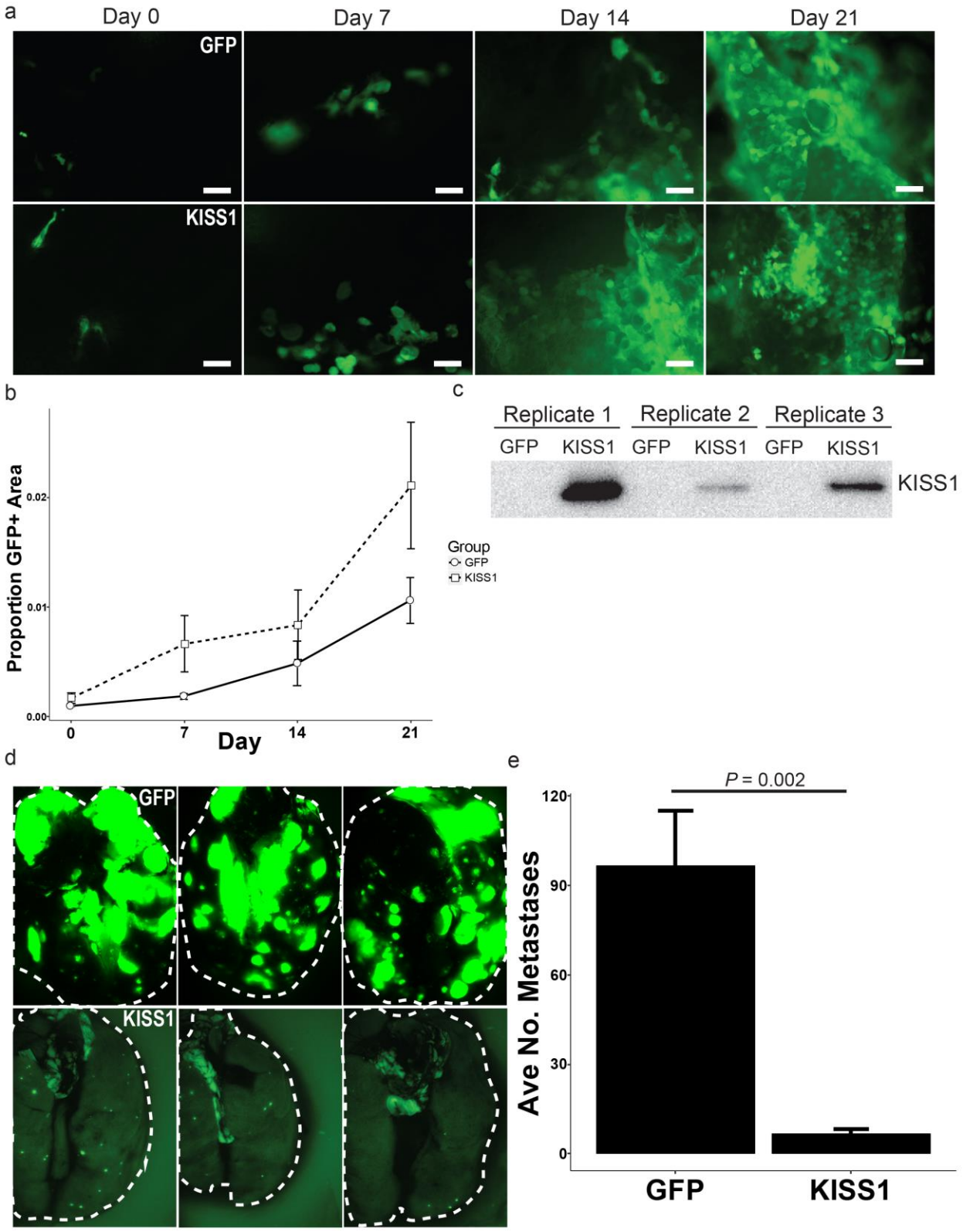

Figure 3-3 Comparison of KISS1 Growth Suppression in vivo and ex vivo (PuMA). (a) Representative images of growth of GFP control (top) or KISS1 expressing (bottom) C8161.9 melanoma cells at days 0,7,14 and 21 in the PuMA. Scale bar for fluorescent image is 50 μm. (b) Quantification of PuMA experiments by image analysis. No significant differences. n = 3 (c) Immunoblot for KISS1 from conditioned media from either GFP control or KISS1-expressing melanoma cells grown in the PuMA demonstrates KISS1 remains expressed in the PuMA to D21. (d) Representative images of gross lungs containing vector control (top) or KISS1 expressing (bottom) C8161.9 melanoma cells five weeks after tail vein injection demonstrating suppression of lung outgrowth by KISS1 in vivo. n = 5 (e) Quantification of gross lung metastases.

Discussion

While the PuMA assay did not faithfully replicate what we had observed *in vivo* for KISS1-expressing cells, the data set obtained afforded an opportunity to refine the imaging workflow so that future experiments would be more readily analyzed. Objective and quantitative analysis of images containing data from a range of focal planes is difficult due to variations in signal intensity and distribution. We recognize all microscopy methods have unique strengths and limitations [35, 157, 158]. Methods such as confocal microscopy may not suffer as much from large variations in signal intensity. Indeed, this workflow is not intended to substitute one microscopy for another. Rather, our goal was to improve the capacity for epifluorescence microscopy data, nearly ubiquitous in many labs, to be more objectively quantified. Automating image selection may also help reduce (remove) bias by applying a standardized method to image selection for analysis, rather than leaving the decision to a single observer. While we acknowledge that our initial stratification was empiric and could be a source of potential bias, we also demonstrate that the complex signal differences between analyzable and unanalyzable image parameters were quantifiable and could be used to objectively select of images useful for automated analysis in future experiments. This platform mirrors other machine learning approaches such as non-negative matrix factorization, Random Forest classification, or Potts models [159, 160].

Using this workflow, we measured growth of disseminated cancer cells as a function of in-focus GFP-positive surface area in lung tissue. This method has immediate utility in the PuMA, but might also be applied to *in vivo* data such as the quantification of luciferase signal in whole animals with metastases [158]. While our model identified a number of features within an image to be significant in stratifying images, the features identified for other types of data are likely to vary greatly. This flexibility lends itself to the objective analysis of a potentially broad range of biological imaging data. For example, comparing relative roundness versus spindle morphologies could assess epithelial-to-mesenchymal transition, which contributes to some cells' metastatic or invasive potential [161, 162]. Additionally, using multiple features of the ROI creates a stronger tool for distinguishing in-focus from out-of-focus ROI than would a single modality, such as a gradient based on pixel saturation alone [163].

Despite the disappointment that PuMA did not mimic *in vivo* results in the C8161 KISS1 melanoma model, the results may still have provided clues regarding mechanism of action. KISS1-expressing cells still proliferated. Since we previously showed that C8161 cells do not express the KISS1 receptor GPR54 [28], eliminating autocrine feedback of KISS1 on this receptor as a potential mechanism, the hypotheses related to paracrine mechanisms or alternative feedback [164] are supported. Three possibilities exist for the lack of consistency between the *in vitro* and *in vivo* data: (1) a factor required to suppress growth of KISS1-expressing cells is missing in PuMA; (2) a molecule that promotes growth of KISS1-expressing cells is 'uncovered' in PuMA; or, (3) KISS1 suppresses at a step other than proliferation at the secondary site and that step is not measured by PuMA. Perhaps the secretion of KISS1 alters the microenvironment *in vivo*

such that dormancy is induced in disseminated melanoma cells? While effects on lymphoid derived immune cells are unlikely due to the fact that suppression is observed in nude mice lacking fully developed T cells, potential suppressive effects from KISS1 on myeloid derived immune cells, such as macrophages, have not been ruled out. Such a result might also explain the absence of suppression in *ex vivo* models if such suppressive immune cells are not recruited in the short time disseminated cancer cells circulate before collection of the lungs for PuMA culture *ex vivo*. These data, taken together with results from all of the other assays measuring steps of metastasis *in vitro,* emphasize that the whole is indeed more than the sum of its parts; measuring steps of the metastatic cascade independent of their context *in vivo* provides observations which may not necessarily be representative of the entire process of metastasis. The ability of this system to engage varied and challenging datasets has potentially broad applications within metastasis research.

Supplementary Data

Supplemental 1 is a comprehensive step-by-step protocol for the use of the workflow and the scripts which are freely available:

https://drive.google.com/drive/folders/1zmjp_VW_Pnw7BdyeAut36DS1J6AoJ-QG?usp=sharing

This protocol also includes a troubleshooting guide for commonly encountered errors.

Figure 3-4: Image Selection and In-Focus Particle Identification

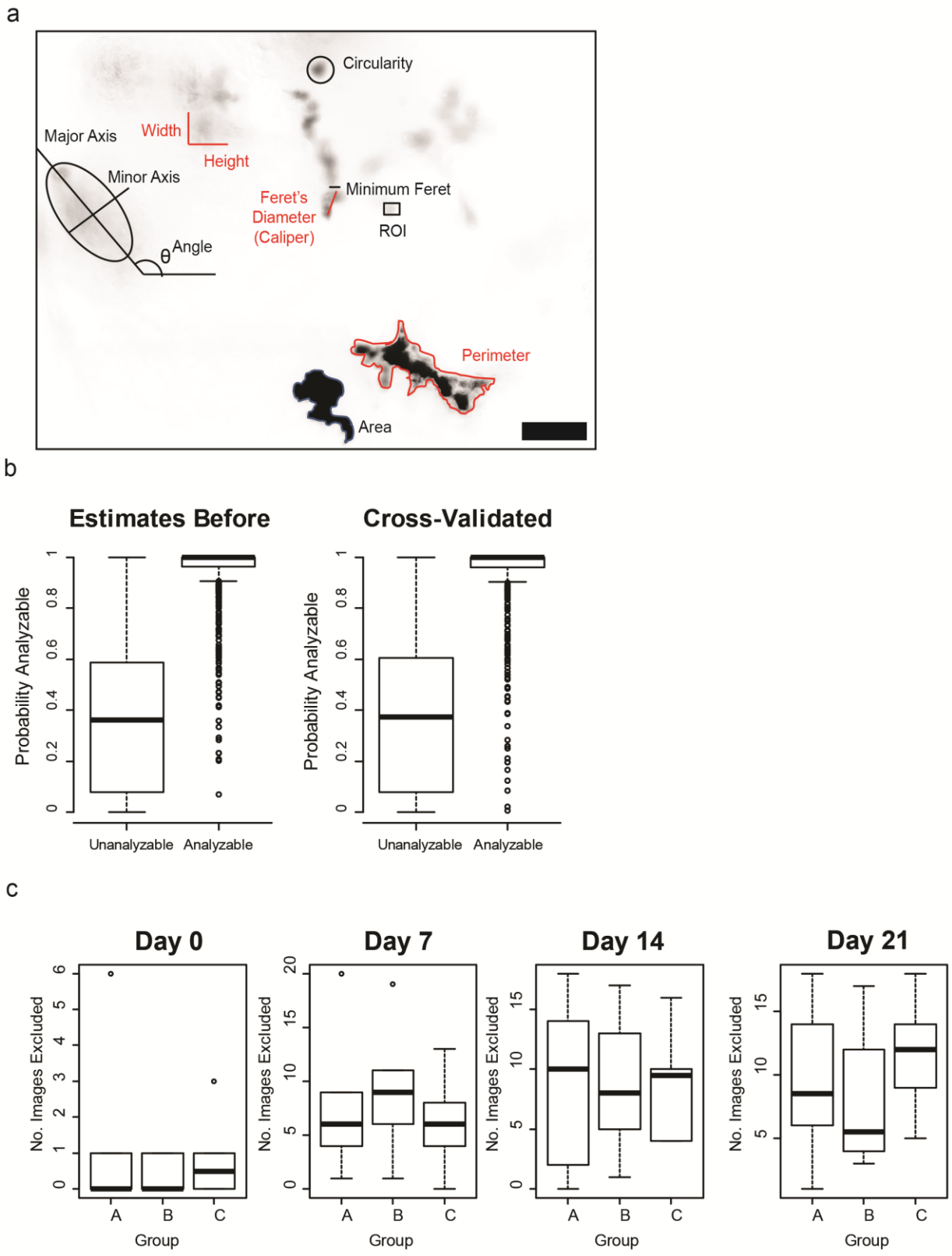

Figure 3-4 Region of interest (ROI) features and statistical validation of image stratification mode. (a) Illustration of measurable and statistically significant (red) or not (black) features of ROIs between analyzable and unanalyzable images. These features were used to stratify analyzable images used for further analysis from unanalyzable images (excluded). Scale bar is 50 μm. (b) Cross-validation results from logistic regression comparing test set and new sample sets. (c) Comparison of mean number of excluded images from three biologically distinct groups for each time point. One-way ANOVA followed by Tukey's post hoc test found no significant differences were found between groups suggests all groups were excluded equally. For each group, degrees of freedom = 2 and residuals = 15.

Chapter 4 **– ITIH5 as an Inhibitor of Pancreatic Cancer Metastasis**

Introduction

Pancreatic ductal adenocarcinoma (PDAC) is a deadly cancer; liver metastasis is common and on average only two percent of patients diagnosed with metastatic disease survive five years or more. In order to identify genes contributing to metastasis of PDAC to the liver, we performed a genome-wide screen in a non-metastatic human PDAC cell line, S2-028 [29]. This screen identified two suppressors of pancreatic cancer metastasis, one of which was Inter-Alpha-Inhibitor-Heavy-Chain 5 (ITIH5). We used shRNA knockdown and overexpression experiments were performed in human PDAC cell lines (MIAPaCa-2, BxPC-3, Panc-1 and SUIT2 derivatives S2-028 and S2-007). These data revealed that expression of ITIH5 correlated with decreased cell migration, invasion and liver metastasis, but had only a marginal effect on growth of the primary tumor *in vivo*. Knockdown of ITIH5 in S2-028 cells increased migration, invasion, mesenchymal shape and liver metastasis. Conversely, in the highly metastatic human PDAC cell line S2-007, which has low endogenous expression of ITIH5, re-expression of ITIH5 reduced cell motility, invasion, and liver metastasis and was correlated with a change to an epithelial morphology. Interestingly, observations from normal physiology show similar correlations between reductions in cell motility/invasion and expression of ITIH5. For example, ITIH5 expression increases in the murine placenta during gestation [165], and in humans ITIH5 is expressed in what appears to be the syncytiotrophoblast of term placenta after endometrial invasion has ceased [29].

Decreased expression of ITIH5 has been reported in a number of other human cancers, including breast [54], lung [62], bladder [61], stomach [66], colon [166], acute

myeloid leukemia [65] and ependymoma [64]. In breast cancer, expression of ITIH5 has been correlated with changes in expression of integrins, other tumor suppressors and changes in the activation of small GTPases [68]. Such changes in the activation of GTPases may help explain the observed changes in morphology upon ITIH5 expression but a definitive mechanism of metastasis suppression remains to be elucidated.

ITIH5 is a secreted protein and is thought to play a role in stabilization of the extracellular matrix like other members of the Inter-alpha-trypsin inhibitor family [56], but relatively little is known about the localization of ITIH5. To our knowledge, there have been no reports describing the subcellular localization of ITIH5 in PDAC. Furthermore it is known that the Inter-alpha-trypsin family of proteins undergo extensive post-translational processing [167], but it was not known if ITIH5 undergoes similar processing or if such cleavage and crosslinking events have any significance with respect to ITIH5's function as a metastasis suppressor. Thus, we began by identifying where ITIH5 is expressed in human PDAC and observed how ITIH5 is processed to understand whether localization or processing have any functional significance in the mechanism of suppressing liver metastasis. Finally, since ITIH5 is a secreted extracellular matrix protein, we tested whether secretion of ITIH5 was required to suppress metastasis by deleting the N-terminal secretion sequence, creating a non-secreted ITIH5 expression construct (ITIH5Δs). Determining the mechanism by which ITIH5 suppresses PDAC liver metastasis may help establish future therapeutic targets related to ITIH5 and ultimately, reduce the morbidity and mortality associated with PDAC liver metastasis.

Methods

Cell lines and cell culture

Human PDAC cell lines (SUIT2 derivative S2-007 and MiaPaCa-2) were cultured in DMEM/F12 (Gibco Cat #11330-032) with 5% fetal bovine serum (FBS) (Cat #S11195, Atlanta Biologicals, Atlanta, GA), 1% glutamine (Gibco, #25030-081) 0.25% non-essential amino acids (Gibco, #11140-050) and 1.5 and 1.0µg/mL Puromycin respectively (Gibco, #A11138-03) in a humidified incubator at 37°C.

Cell Migration (Scratch) Assays

PDAC cell lines were cultured using the conditions described above. Cells were plated in 6 well plates (Corning, Cat #07-200-83) and grown to near confluency after 48 hours of growth in a humidified incubator at 37°C (1 or 2 million cells). Plates were scratched using a 200µl filtered tip (Avant, Cat#ARS-200) with the plate lid as a guide. Two vertical and equally spaced scratches were made in each well. Plates were then rinsed twice with Phosphate Buffered Saline (PBS) and culture media was replaced before phase contrast imaging using a Nikon Eclipse TS100 Inverted Microscope, QImaging QIClick monochrome CCD camera and Metamorph software. Surface area of the open space between cells was measured using ImageJ software [152] and the Wound Healing Tool macro [168]. For each time point, three images per scratch and two scratches per experimental group were recorded for each experiment. All experiments were repeated at least three times.

Cell fractionation experiments

Cytoplasmic-Nuclear fractions were separated according to the manufacturer's instructions using the NE-PER™ Nuclear and Cytoplasmic Extraction kit (ThermoFisher, #78835). Membrane-Cytoplasmic fractions were separated according to the manufacturer's instructions using the Mem-PER™ Plus Membrane Protein Extraction kit (ThermoFisher, #89842).

Immunoblotting

Cells cultured *in vitro* were lysed using 1X RIPA buffer (Millipore, #20-188) with 1% protease-phosphatase inhibitor (Thermo, #78411) on ice for 15 minutes before centrifuging (13,000 RPM) for 15 minutes. Protein concentration was determined using a BCA assay (Thermo, #23227). Whole cell lysates were denatured using NuPAGE LDS Sample Buffer (Invitrogen, #NP0007) with 10% BME (Sigma, #60-24-2) at 95°C for at least five minutes before separation using either a 4-20% gradient SDS-PAGE gel (Bio-Rad, #567-1039) or a 10% gel (Bio-Rad Acrylamide, #161-0158) and proteins were transferred to PVDF membranes (Bio-Rad, #170-4156), and blocked for at least one hour using 5% milk in Tris Buffered Saline with Tween-20 (TBST). Antibodies were diluted 1:1000 in blocking solution and membranes were allowed to incubate overnight at 4°C (ITIH5: ThermoFisher #PA5-24445, CD44: R&D Systems #BBA10) or for one hour at room temperature (GAPDH, Cell Signaling, #2118). Anti-FLAG M2 HRP conjugated mouse monoclonal antibody (ThermoFisher, #A8592) were used to detect FLAG. Secondary antibodies (Anti-Rabbit: GE #NA934V, Anti-Mouse: GE #NA931V) were

diluted 1:5000 in block and were allowed to incubate for one hour at room temperature in protein block.

Immunoprecipitation from Conditioned Media

Cells cultured *in vitro* were allowed to grow to near confluency for 48 hours. Cells were washed twice with PBS, and media was replaced with fresh media. Cells were allowed to grow for 24-48 hours and conditioned media was collected. Conditioned media was centrifuged at 12,000rpm for 3 minutes at 4°C to remove debris. Supernatant was transferred to clean, pre-chilled microcentrifuge tubes (~1ml/sample). Samples were pre-cleared from nonspecific interactions to agarose beads by adding 10-20ul agarose beads and allowed to incubate with rotation for 1hr at 4°C. Samples were then centrifuged at 12,000rpm for 3 minutes at 4°C and supernatant was transferred to new pre-chilled microcentrifuge tubes. ITIH5 (ITIH5, ThermoFisher, #PA5-24445), Anti-FLAG (ThermoFisher, #F1804-200G), or control antibodies (Cell Signaling, Mouse IgG #5415, Rabbit IgG #2729) were added and allowed to incubate at 4°C with inversion overnight. The next day, 20µl A/G beads per 1 ml were added and allowed to incubate overnight at 4°C as described above. The next day, samples were centrifuged at 12,000rpm for 10 minutes at 4°C to precipitate beads. Supernatant was aspirated and beads were washed with 250µl ice cold PBS and centrifuged at ~3,000rpm at 4°C for five minutes (x3). 20ul loading dye with mercaptoethanol was added to resuspend each bead pellet and samples were boiled for 5 minutes at 95°C. Samples were loaded on gels for immunoblotting as described above.

RhoA Activation Assays

Activated RhoA was detected using an immunoprecipitation based assay (Active Rho Detection Kit, Cell Signaling #8820). Cells were grown in culture, lysed and protein quantified using a BCA assay. 500µg of protein were collected, mixed with GST-Rhotekin-RBD beads and GTP bound proteins were eluted. Positive controls were treated with GTPγS before elution, while negative controls were treated with GTPγS but no GST-Rhotekin-RBD beads were used to bind GTP substrates before eluting. Eluate was ran on a gel and blotted for Rho proteins (#8789), RhoA (#2117) or RhoC (#3430) using immunoblotting described above.

Extracellular Vesicle (EV) Isolation

Exosome purification was performed as previously described [169] with minor modifications. Briefly, cells were grown to 70% confluence at 48hr after plating in 10 cm dishes and washed twice with 1X PBS. Cells were incubated in 7 ml/dish of EV-free medium for 36-48 hours before harvesting media. Cells were centrifuged in conical tubes in table top centrifuge with swing bucket rotor at 300 g for 10 min at 4°C and then transferred to fresh tubes on ice. Supernatant was centrifuged at 2,000 g for 10 minutes at 4°C. Supernatant was transferred to autoclaved 500 ml Nalgene bottles and centrifuged at 16,500 g for 30 min at 4°C in a floor model centrifuge with a fixed-angel rotor. Supernatant was transferred to thin polymer open top tubes (Fisher, #03-126) and centrifuged at 110,000 g (24,300 rpm) in an ultracentrifuge using a swing bucket (SureSpin630 6X16) rotor for 1.5 hours at 4°C. Supernatant was removed and pellets were resuspended in 1 ml ice cold PBS before centrifuging at 110,000 g (24,300 rpm) in

a floor model ultracentrifuge using a swing bucket (SureSpin630 6X16) rotor for 1.5 hours at 4°C. Supernatant was removed and pellet was resuspended in 20-40µl PBS before lysis, protein quantification and western blotting.

Trypan blue cell proliferation assays

To measure cell proliferation *in vitro,* 1.0 x 10^4 human PDAC cells were plated in a 6-well cell culture dish (Corning, Cat #07-200-83) using culture conditions described above. At days 1, 3, 7, 10 and 14 cells were washed with 1X PBS (Gibco #10010-023) and detached using trypsin-EDTA (Gibco #25200-056) until cells were free-floating. An equal volume of media with fetal bovine serum (FBS, Atlanta Biologicals, #S11195) was used to create a single-cell suspension. The concentration of cells was determined using a hemocytometer (Reichert, Cat #Z359629). Both live and dead cells were counted and distinguished by exclusion or passive uptake of trypan blue solution (Sigma, Cat #T8154). Experiments were conducted in triplicate and standard errors were calculated.

Plasmids and viral transduction

The secretion sequence of ITIH5 was removed to create the deleted secretion ITIH5 (dsITIH5) mutant. Deletions and restriction sites were inserted using directional cloning techniques and verified by restriction digest and sequencing. Lentiviral transduction was used to introduce the construct into PDAC cells. DNA was amplified using Gold competent cells. Plasmids were transfected into packaging cells according to Polyplus transfection recommendations using jetPRIME Transfection reagent (Polyplus, #114-15) and Polyplus Buffer (Polyplus, #712-60). This was added to packaging cell

media and transduction was allowed to occur overnight. More media was added at 24 hours and 48 hours after transfection, viral supernatant was collected, precleared using centrifugation and filtered through 0.45 low protein-binding filters (GVS, #09-977-751) and applied to cells. Transductions occurred for 3 days and then cells were allowed to rest in culture media before undergoing puromycin selection for 4 days.

Experimental metastasis assay—intrasplenic injections

In order to measure growth of disseminated pancreatic cancer in the liver, PDAC cells were injected intrasplenically into 6-8 week old athymic Nude-*Foxn1*^{nu} mice (Envigo/Harlan) and were allowed to circulate and seed the liver via the portal circulation for two minutes. A splenectomy was subsequently performed to remove intrasplenic tumor burden and allow for outgrowth of liver metastases. These procedures were performed as previously described [24, 29]. For S2-007, 5 x 10^5 were injected in 100µl Hanks Balanced Salt Solution (HBSS, Gibco, #14175-103) and allowed to grow for 4 weeks, or until the mouse was moribund and required euthanasia.

Quantification of Metastases

Quantification of gross liver metastases was accomplished with the assistance of a Nikon SMZ1500 Stereomicroscope and 1-10mm reticle. Length and width of each metastasis was measured. All lobes of the liver were counted and both superior and inferior surfaces of the liver were assessed for metastases. Metastases visible from both sides of the liver were only counted once. Histologic metastases were measured from hematoxylin and eosin (H&E) stained paraffin sections. Livers were fixed in formalin

(Fisher, # SF-98-4) for at least 24 hours before dehydrating and paraffin embedding. Sections were cut on a microtome to 7 µm and H&E stained using standard methods. Five H&E images were taken at 4x magnification from each liver and three mice per group were assessed. Area of metastases and liver visible were recorded using the multi-point tool in ImageJ. Percentage of liver area occupied by metastases was recorded and compared between experimental groups.

Statistical Analysis

All statistical analysis was carried out using R software [154]. For comparisons between groups, one-way ANOVA was used followed by Tukey's *post hoc* test.

Results

Expression, localization and peptide processing of ITIH5 in human PDAC

In breast cancer, ITIH5 is a secreted extracellular matrix protein with distinct functional domains [54, 170]. The Inter-α-Inhibitor Heavy Chain Family (IαI) members are typically cleaved and covalently linked by chondroitin sulfate [167]. Consistent with this pattern, ITIH5 contains a cleavage site at D681-V686 [54], dividing the ~105kDa protein into ~75kDa and ~29kDa fragments. The ITIH5 antibody used binds an epitope on the N terminus of the cleavage site and the FLAG epitope is present at the C terminus of the protein (Fig. 4-1a), so if ITIH5 were cleaved, we would expect to see bands detecting ITIH5 with this antibody at ~75 (cleaved N fragment), ~105 (full length ITIH5) or ~150kDa (covalently linked 75kDa fragments). Similarly, we would expect to see fragments at ~105

(full length ITIH5) or ~29kDa (cleaved C fragment) using our anti-FLAG antibody (Fig. 4-1a).

Figure 4-1: ITIH5 is secreted and cleaved extracellularly in PDAC cells.

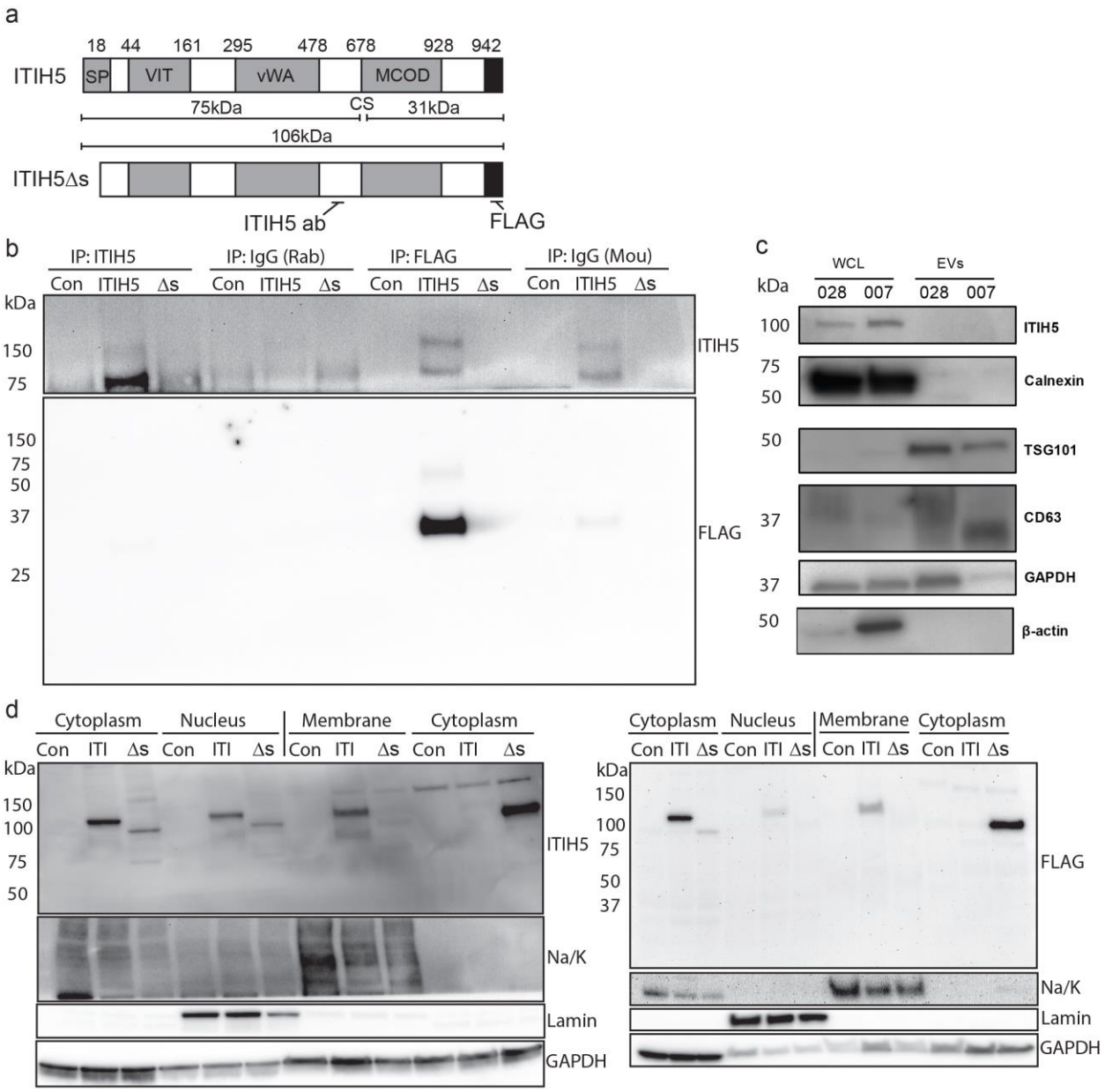

Figure 4-1 Expression and localization of ITIH5 and non-secreted ITIH5Δs. A) Organization of ITIH5 domain structure labeled by amino acid number for full length ITIH5 (ITI) and secretion-deficient (Δs) expression constructs, domain map adapted from Himmelfarb et al, 2004. Grey bars: secretion signal peptide (SP), vault protein inter-alpha-trypsin domain (VIT), von Willebrand type A domain (vWA), cleavage site (CS), multicopper oxidase domain (MCOD). Black bar: FLAG tag (FLAG). B) Immunoprecipitation of extracellular ITIH5 from conditioned media using ITIH5 antibody (binds on N terminal side of cleavage site at AA578-606) and FLAG antibody (binds on C terminal side of cleavage site after end of ITIH5 open reading frame). C) Western blotting of exosome preparations (SIZE RANGE) for ITIH5. D) Western blotting of ITIH5 in cellular fractions enriched for either cytoplasm/nucleus or membrane/cytoplasm. Abbreviations: Na/K: Sodium/Potassium ATPase. GAPDH: Glyceraldehyde-3-phosphate dehydrogenase.

We hypothesized that the secretion of ITIH5 would be required for the suppression of pancreatic cancer metastasis and first sought to characterize the localization of ITIH5 in PDAC. We expressed both secreted (ITIH5) secretion-deficient ITIH5 (ITIH5Δs) constructs in the highly metastatic and low endogenous ITIH5-expressing human PDAC cell lines S2-007, and MiaPaCa-2. Levels of expression were similar to endogenous levels of ITIH5 observed in cultured pancreatic epithelial cells [29]. In the secretion mutant ITIH5Δs, secretion into conditioned media was inhibited (Fig. 4-1b). Interestingly, ITIH5 appears cleaved extracellularly as indicated by the absence of the 105kDa fragment and predominance of the 75 and 29kDa fragments in conditioned media of the ITIH5-expressing cells. The consensus cleavage sequence (DPHFVV) is predicted to be cleaved by chymotrypsin [167] (DPHF│VV), but may also be cleaved by a number of putative serine proteases at varying amino acid positions. In this case, the small C terminal (29kDa) fragment appears to run at a higher molecular weight due to the 17aa added after the ORF (9aa plus 8aa FLAG tag) before the STOP codon in the expression construct. Seeing that ITIH5 is secreted extracellularly in PDAC, we looked to see if ITIH5 was secreted into extracellular vesicles. However, ITIH5 does not appear to be secreted into extracellular vesicles (mean particle size of 155nm, Fig. 4-1c), but may be secreted directly from Golgi vesicles.

Next, we performed cellular fractionation experiments to understand the intracellular localization of ITIH5. Reagents which separated the cytoplasmic fraction from the nuclear fraction, or which separated the cytoplasmic fraction from the membrane fraction (or potentially membrane-bound fraction) were used to assess the cellular

compartments for ITIH5 expression. Furthermore, the molecular weight of the ITIH5 expressed was detected with both the anti-ITIH5 and anti-FLAG antibodies, allowing us to detect potential protein processing events such as peptide cleavage or dimerization.

Interestingly, the ~75kDa and ~29kDa fragments did not appear intracellularly. Instead, ITIH5 appeared at its full-length molecular weight of ~105kDa using both the ITIH5 and FLAG antibodies (Fig. 4-1d). ITIH5Δs runs at a slightly lower molecular weight due to deletion of the 18aa secretion sequence. Crosslinking of the two ~75kDa Inter-alpha-trypsin N terminal fragments into a ~150kDa dimer does occur and should be detectable using the anti-ITIH5 antibody. Indeed, a ~150kDa band is visible in the cytoplasmic fraction when separated from the membrane fraction. This suggests that ITIH5 may also be cleaved intracellularly, and that the ~75kDa fragment is likely cross-linked to short chains of chondroitin sulfate or hyaluronic acid to create the ~150kDa dimer in an organelle such as the Golgi. We were not able to detect ~29kDa fragment intracellularly, perhaps due to degradation during processing. ITIH5 is also visible in the nuclear fraction at the ~105kDa molecular weight. Because of the large size of ITIH5, transport into the nucleus is anticipated and ITIH5 indeed contains at least three predicted nuclear localization sequences (aa500-526, aa732-741, and aa890-919), although it is not currently known which potential nuclear localization sequence is required for nuclear localization.

Expression of ITIH5 Affects Cell Morphology and Motility

Expression of ITIH5 has been shown to alter cell morphology *in vitro* [68]. We expressed ITIH5 in highly metastatic human PDAC cells and observed effects similar to

those described (Fig. 4-2a). The effects were most dramatic in the S2-007 cells. Interestingly, expression of ITIH5Δs showed an indistinguishable phenotype (Fig. 4-2a), despite the fact that this molecule is not secreted (Fig 4-1b). These data imply that an intracellular effect could contribute to the metastasis-suppressive effects of ITIH5.

The pancreatic cancer cell lines in these experiments share activating mutations in KRAS, inactivating mutations in p53 and inactivating mutations in p16 (CDKN2A) [171]. In order to understand the mechanism of metastasis suppression by ITIH5, we first looked to see whether ITIH5 expression affects cell proliferation *in vitro.* We found that expression of either ITIH5 or ITIH5Δs did not significantly affect rates of cell proliferation or cell death at steady state (Fig. 4-2b). We have previously reported that expression of ITIH5 was correlated with decreased cell motility [29]. We tested the effect of expressing ITIH5Δs and found that intracellular ITIH5 also reduced cell motility as measured using the wound healing assay (Fig. 4-2c, 4-2d). Together, these results suggest that the mechanisms by which ITIH5 induces a rounded cell morphology and slows cell motility does not require secretion, but appears to be due to an intracellular role of ITIH5. Therefore, the metastasis-suppressing influence of ITIH5 could be due to intracellular effects.

Figure 4-2: Expression of ITIH5 changes cell morphology and migratory capacity.

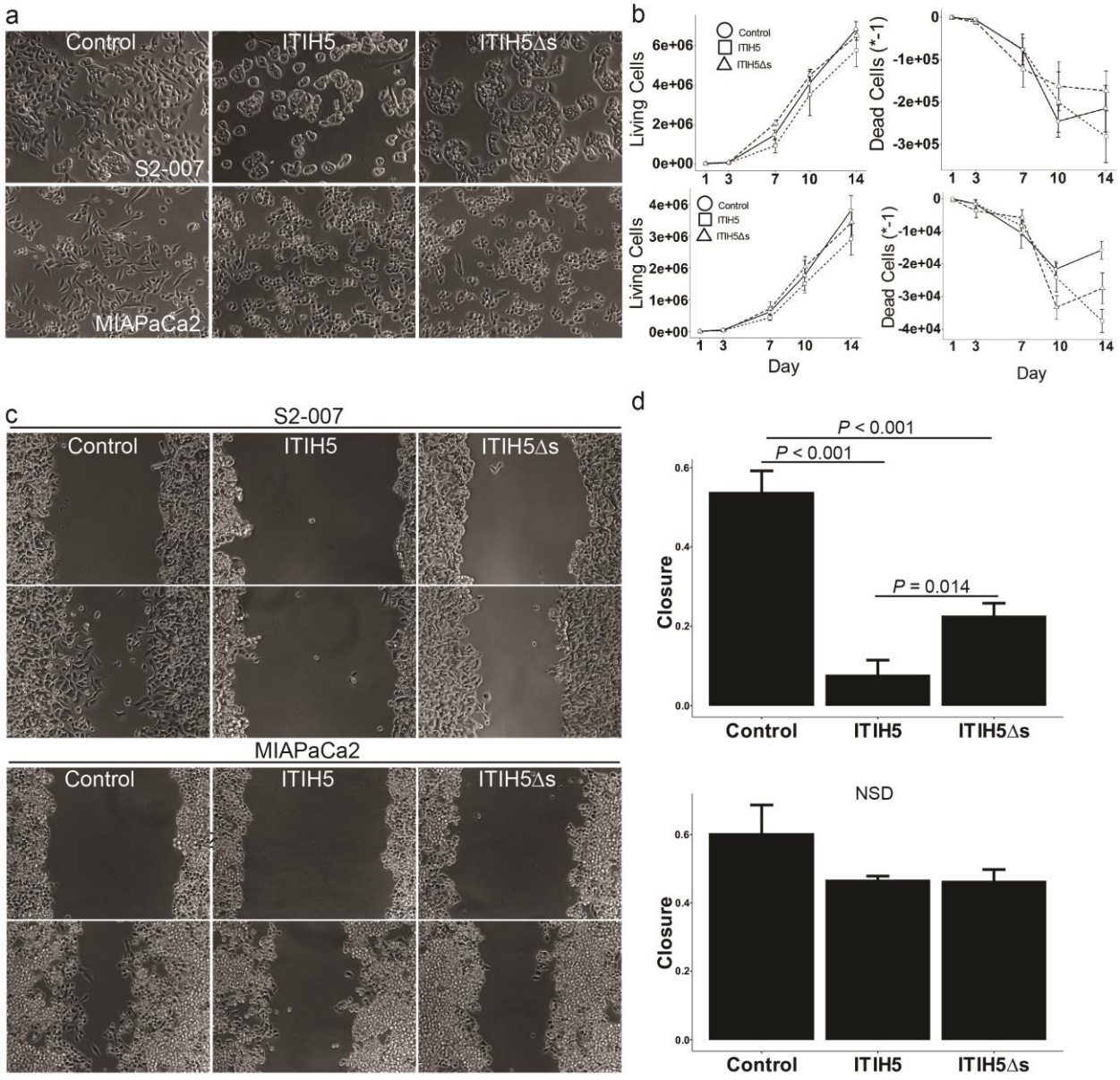

Figure 4-2 Assessment of secreted (ITIH5) and non-secreted (ITIH5Δs) expression on PDAC cell morphology, proliferation, and migration. A) Expression of extracellular and intracellular full length ITIH5 and intracellular only secretion-deficient ITIH5Δs in metastatic and low-ITIH5 expressing human PDAC cell lines S2-007, and MiaPaCa-2 is correlated with rounded cell morphology and tight epithelial-like clustering. B) Expression of intracellular and extracellular ITIH5 or intracellular only ITIH5Δs cause no changes in cell proliferation or cell death in vitro. C) Expression of both ITIH5 and ITIH5Δs reduced cell motility in an in vitro wound healing/scratch assay. D) Quantification of results from wound healing assay, measurement of percentage wound closure after elapsed time.

Effects of Intracellular ITIH5 in vitro and in vivo

Next, we tested whether secretion of ITIH5 was necessary for suppression of liver metastasis. We injected human PDAC cells expressing ITIH5 or ITIH5Δs into 6-8 week old athymic nude mice intrasplenically and cells were allowed to circulate and seed the liver via the portal vein. Strikingly, we saw that non-secreted ITIH5Δs also suppressed liver metastasis, indicating an intracellular role for ITIH5 in metastasis suppression (Fig. 4-3a, b). Animals bearing disseminated tumors expressing ITIH5 or ITIH5Δs showed reduced number of macroscopic metastases (median, Control = 13, ITIH5 = 5.5 and ITIH5Δs = 3), although only comparison between Control and ITIH5Δs groups reached statistical significance (P = 0.029). This could be due to a single large potential outlier in the ITIH5 group (28 metastases). Size of macroscopic metastases were also reduced by expression of either ITIH5 or ITIH5Δs as measured by the sum of the longest dimension of each metastasis (median, Control = 21.5, ITIH5 = 7, ITIH5Δs = 4). Expression of either ITIH5 or ITIH5Δs also reduced the number (average, Control = 3.3, ITIH5 = 1.7, ITIH5Δs = 1.3) and area occupied (average percent liver occupied by metastases, Control = 0.19, ITIH5 = 0.06, ITIH5Δs = 0.07) by histologic metastases (Fig. 4-3c, d). As lung metastases are possible in this assay from PDAC cells passing through the liver and lodging in lung capillaries, we also assessed the lungs for metastases. No gross metastases were visible on the surface of the lung, but in the vector control and ITIH5Δs groups, metastases were present in the lung histologically. There was no statistically significant difference between the number of lung metastases in these two groups (Fig. 4-3e, f). These results could indicate some tissue specificity in growth suppression by ITIH5. For example, it is known that lung is a more hospitable microenvironment for PDAC metastases as compared to

the liver [172], which might render the metastasis suppressive effects of ITIH5 less apparent. Further sampling is underway to determine whether this difference was due to inadequate sampling or a true difference in biology.

Figure 4-3: Intracellular ITIH5 (ITIH5Δs) suppresses liver metastasis.

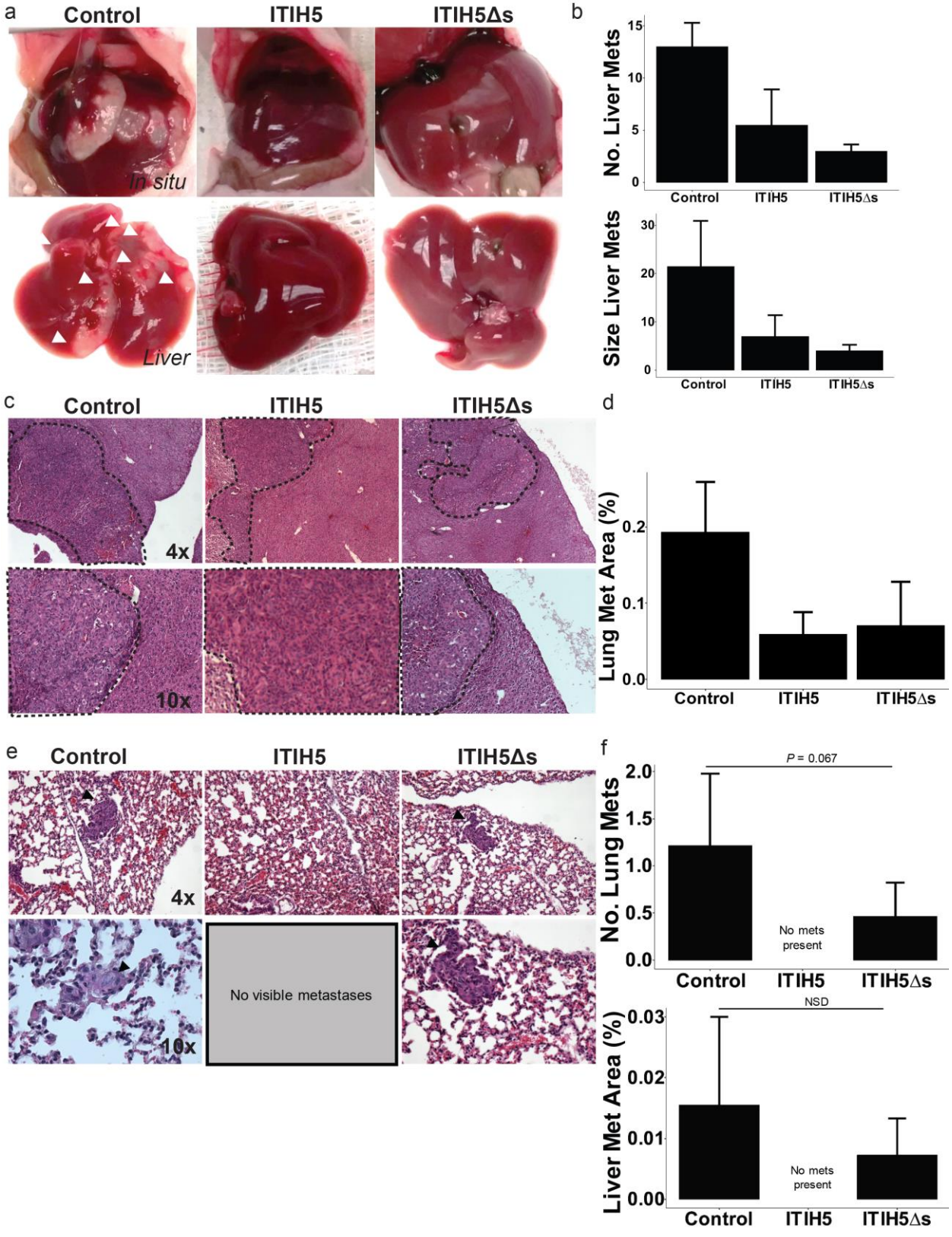

Figure 4-3 Assessment of secreted (ITIH5) and non-secreted (ITIH5Δs) expression on metastatic efficacy of highly metastatic S2-007 cells. A) Images of livers in situ and ex vivo from intrasplenic experimental metastasis assay. Human PDAC cells (S2-007) were transduced with control vector, ITIH5 or ITIH5Δs. B) Quantification of median number and median size of gross liver metastases. C) Low and high magnification of histologic sections of liver containing metastases. D) Quantification of area containing liver metastases. E) Low and high magnification images of lung sections from experimental metastasis assay. F) Quantification of lung metastases from intrasplenic injection.

Effects of ITIH5 expression on Rho GTPase Signaling

We observed that expression of both ITIH5 and ITIH5Δs in human PDAC cells induced a rounded, epithelial-like cell morphology. Activation of the small GTPases of the Rho family are responsible for mediating changes in cell morphology and migration [173], phenotypes both affected by expression of ITIH5 (Fig. 4-2a, c). Previous work has shown that expression of ITH5 increases activation through the small GTPase RhoA [68]. RhoA is thought to have a tumor-suppressive role in cancer [174], although data also exist supporting a potentially oncogenic role [175]. We hypothesized that expression of ITIH5 might be altering activation through RhoA, and thereby altering both cell morphology and metastatic efficacy.

Furthermore, ITIH5 is predicted to bind hyaluronic acid (HA), which can also signal through Rho GTPases [176]. CD44 is a receptor for HA [177] and also a potential marker of cancer stem cells (CSCs) and prognosis in PDAC [178]. Given that binding of CD44 to HA can activate Rho GTPases downstream [179], we first asked whether ITIH5 might affect expression of CD44 upstream of RhoA to modulate activation of RhoA (Fig. 4-4a). However, it does not appear that either secreted ITIH5 or non-secreted ITIH5Δs alter the expression of CD44in MiaPaCa-2 cells. Next, we tested whether expression of ITIH5 might alter the activation of Rho GTPases using a Rhotekin-RBD bead-mediated pulldown assay for activated Rho. First, we validated the assay using a pan-Rho antibody

and demonstrated that no signal was detected when the samples were activated with GTPγS and the Rhotekin-RBD beads were omitted (negative control), that GTPγS-activated samples could be detected when pulled down with Rhotekin-RBD beads (positive control), and that therefore GTP-bound Rho was detectable (Fig. 4-4b). We hypothesized that expression of ITIH5 might increase activation of RhoA and thereby mediate changes in cell morphology and metastatic efficacy. However, when we assessed levels of active (GTP-bound) RhoA in S2-007 and MiaPaCa-2 cells, we did not see significant increases in activated RhoA in the metastasis-suppressed ITIH5 and ITIH5Δs groups (Fig. 4-4c). We also observed no significant change in GTP-bound (active) RhoC that might correlate with observed metastatic efficacy (Fig. 4-4d). As a negative result, this RhoC experiment was not repeated and so interpretation may be limited. In summary, we found no consistent difference in activation of RhoA or RhoC between control cells and ITIH5 or ITIH5Δs-expressing cells. Together, these data suggest that despite the activation of RhoA observed after expression of ITIH5 in breast cancer [68], neither HA/CD44 signaling nor direct activation of RhoA are likely responsible for the metastasis-suppressing role if ITIH5 in PDAC.

Figure 4-4: Intracellular ITIH5 Expression Does Not Affect RhoA/CD44 Signaling

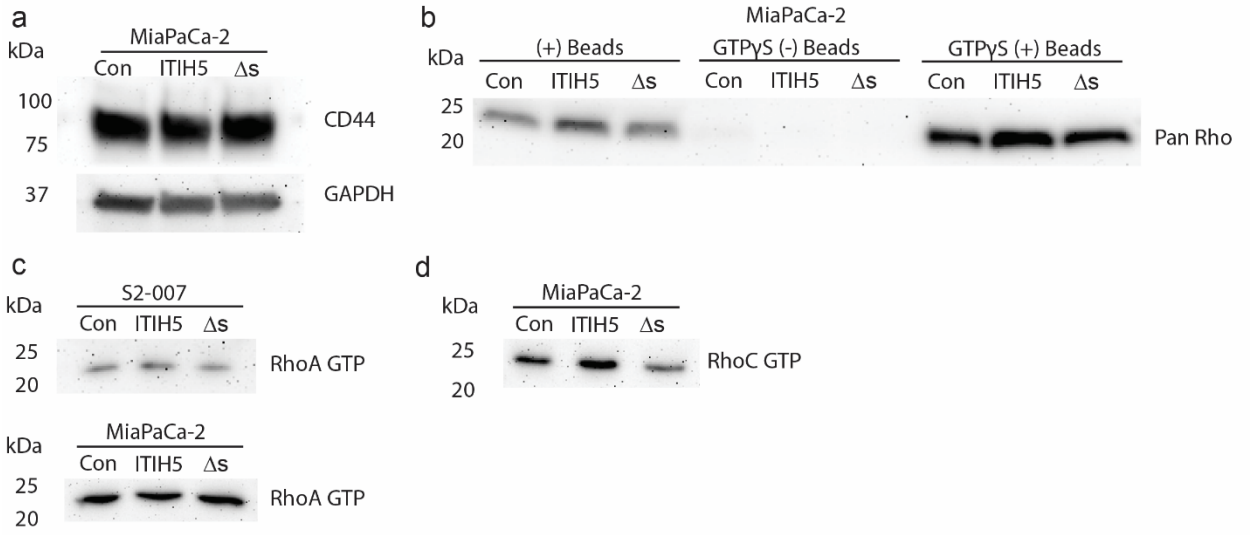

Figure 4-4 Comparison of CD44 expression and activation of Rho GTPases with expression of ITIH5 and non-secreted ITIH5Δs in human PDAC. A) Western blot for CD44 and GAPDH in PDAC. B) Validation of GTP pulldown assay showing Rhotekin-RBD bead mediated pulldown of GTP bound (active) Rho (pan Rho antibody), samples activated with GTPγS but omitting bead pulldown (negative control), and samples activated with GTPγS pulled down with Rhotekin-RBD beads (positive control). C) Assessment of RhoA activation (GTP-bound RhoA) in human PDAC cells (S2-007 and MiaPaCa-2) transfected with control vector, ITIH5 and ITIH5Δs. D) Assessment of activated (GTP-bound) RhoC in MiaPaCa-2 cells.

Discussion

Expression of ITIH5Δs in S2-007 cells slowed cell migration, reduced liver metastasis following intrasplenic injection into athymic mice, and was associated with an epithelial morphology. Effects of expressing ITIH5Δs mirrored those of expressing full-length, secreted ITIH5. Together, these data suggest that ITIH5 attenuates PDAC metastasis via an as-yet unidentified intracellular mechanism.

We have shown that secretion of ITIH5 is not necessary to suppress liver metastasis in PDAC, suggesting that there may be an intracellular role for ITIH5 in suppressing metastasis. This result was unexpected, as most of what is known about the biology of the inter alpha trypsins (IαI) has focused on their extracellular role, due to their binding of hyaluronic acid (HA) [180], the fact that they are secreted and their structural similarity to serine protease inhibitors. However, this binding to HA may be to short HA polymers which are present intracellularly [167] and not only the multi-kilodalton HA polymers that add structure and hydrophilicity to the extracellular matrix (ECM). Furthermore, we provide what we believe to be the first evidence that ITIH5 is cleaved extracellularly, processed into fragments of differing molecular weights and is localized in both the cytoplasm and nucleus in human PDAC. These observations regarding the subcellular localization of ITIH5 are novel and further work will be required to understand the functional significance of this localization and processing with respect to metastasis suppression. At present, both cytoplasmic and nuclear localization of ITIH5 were observed in both metastasis-suppressed groups (ITIH5 and ITIH5Δs), so it is unknown

whether cytoplasmic, nuclear, or both localizations are required for suppression of metastasis.

Although this result was somewhat surprising, intracellular roles of ECM proteins are not entirely unknown in cancer. For example, MUC1 is a component of the ECM and also acts intracellularly to affect cell signaling and gene transcription [181]. Indeed, intracellular ITIH5 caused similar changes in cell morphology, migration and suppression of PDAC metastasis as secreted ITIH5, strongly suggesting an intracellular mechanism of metastasis suppression. While we did observe changes toward a rounded, epithelial-like phenotype in PDAC just as was observed in breast cancer [68], but we did not observe similar activation of the tumor suppressor RhoA. These differences may be due to tissue-specific effects of ITIH5, or perhaps the changes in morphology are due to changes in expression of other regulators of cell morphology, such as integrins. In breast cancer, ITIH5 was shown to alter expression of integrins, presenting another potential but unassessed candidate to explain the observed changes in PDAC morphology. Furthermore, we did not observe changes in expression of CD44, which also binds HA to activate RhoA signaling and may serve as a cancer stem cell marker in PDAC [182]. In any case, these data suggest that in PDAC, neither activation of RhoA nor modulation of CD44 expression is required for suppression of liver metastasis.

We observed that both secreted ITIH5 and intracellular ITIH5Δs expression in highly metastatic human PDAC cells is sufficient to suppress growth of both gross and histologic liver metastasis. This could suggest that ITIH5 suppresses the growth of PDAC cells within the liver, or that ITIH5 reduces the ability of disseminated cells to enter the liver, and thereby reduces the number of metastatic colonies. In these same experiments,

we did not observe any development of gross metastases in the lungs of mice with liver metastases. We did however observe the development of histologically apparent metastases in the lungs of mice injected with either control or ITIH5Δs-expressing cells. We do not currently know whether the absence of lung metastases in the ITIH5-expressing cells is due to inadequate sampling, or a true difference in biology. In the lung, we did not observe any difference in the number or size of lung metastases between vector control cells and ITIH5Δs-expressing cells. This may be due to the fact that the lung is more easily colonized by PDAC cells than the liver [172], and so the metastasis-suppressing effect of ITIH5 is less apparent in this tissue. Understanding the intracellular mechanism of PDAC metastasis suppression by ITIH5 could reveal new therapeutically targetable pathways that could slow the progression of disease in patients with PDAC metastases to the liver and ultimately improve the outcome of patients with liver metastases.

Chapter 5 **– Summary**

Here, we have explored the biology of metastasis through the role of two tumor suppressors, KISS1 and ITIH5, and how they suppress metastasis in the lung and the liver respectively. Understanding regulators of lung and liver metastasis are certainly relevant to metastases developing in these organs from a number of human cancers, but what might these data mean more broadly for research in the biology of metastasis and how might such data affect patients with metastatic cancer?

For the metastasis suppressors, two main applications in humans arise in cancer detection and cancer treatment. With respect to cancer detection, we observed that high expression of ITIH5 in primary PDAC correlated with extended survival time. Surgical resection of primary PDAC via pancreatoduodenectomy (Krausch-Whipple procedure) presents several challenges for both the patient and the surgeon. For the surgeon, the procedure tests both the physical and mental energy of the surgeon, often requiring several hours due to the deep location of the pancreas, its proximity to critical vascular structures and variation in gastrointestinal anatomy and tumor location. For the patient, the pancreatoduodenectomy, commonly referred to as simply the “Whipple,” has a high morbidity [183], marked by long recovery times and potentially severe complications. If ITIH5 is a marker of patients who are likely to have increased survival after pancreatoduodenectomy, might then ITIH5 expression be part of a panel of biomarkers to stratify patients who might benefit from the procedure and spare those who are unlikely to benefit from it excessive morbidity?

With respect to treatment of metastatic disease, if the mechanism of metastasis suppressors like ITIH5 and KISS1 could be understood, a molecular target in the pathway

might be revealed that could be targeted therapeutically. For example, we observed robust suppression of melanoma cells expressing KISS1 *in vivo,* but KISS1 failed to suppress disseminated cancer growth in the lungs grown in the PuMA *ex vivo.* If the factor responsible for this difference in KISS1 effects on cancer cell growth were discovered, perhaps a drug could be used to either prevent outgrowth of disseminated cancer at a secondary site like the lung. Understanding the biology of metastasis would be especially important for developing treatments for highly metastatic but mitotically indolent tumors, such as some neuroendocrine tumors, where conventional chemotherapies are not effective. In this case, targeting metastasis would provide a new treatment for a disease which is currently difficult to prevent further progression. Stopping spread from the primary before colonization of new organs or preventing cancer's outgrowth at sites of dissemination could confine cancer treatment to that of a localized or chronic disease respectively.

Genes guiding processes like cell proliferation, migration and resistance to cell death are critical for the development of multicellularity. It would seem that such genes are also the Achilles' heel of multicellular organisms when they are commandeered by cancer as neoplastic doppelgangers. For example, in normal physiology, KRAS regulates proliferation in the developing brain [184], even though KRAS is probably better known as one of the pillar mutations in the progression of pancreatic cancer [185]. Likewise, KISS1 regulates the secretion of neuropeptides in the hypothalamus [186] and ITIH5 expression is associated with tendon development in normal physiology [187] but both of these genes are strong suppressors of cancer metastasis and curiously, both are expressed in pancreatic islets and the brain (hypothalamus and hippocampus) [29, 54,

65, 151, 188]. While it is not surprising that the same genes perform similar tasks in normal physiology and cancer (e.g. regulating proliferation), it does raise the question as to how cancer commandeered these genes. One possible explanation for the shared expression of many metastasis suppressors in both the β cells of the pancreas (e.g. KISS1, HMP-19, and ITIH5) and in the brain is that both the hypothalamus and β cells share genes which were used during evolution for both the development of the brain and the pancreas. While the brain and the pancreas do not share a developmental origin, they have converged on the use of the same genes for similar required processes like microvesicle assembly [189], neuropeptide release, cell adhesion [190], and transcriptional regulation [191]. This therefore may help explain shared gene expression programs between apparently different tissues [192].

Metastasis is often viewed as the pinnacle of tumor progression. Most likely, this is owed to the fact that many patients with the late stage cancer have metastases and that primary tumors which metastasize often show aggressive malignant features such as high proliferative indices, invasion and local recurrence. Metastasis is a hallmark of malignant tumors [193, 194], notwithstanding notable exceptions such as desmoid tumors and glioblastoma, which, while non-metastatic are undoubtedly malignant due to their propensity to invade locally and recur. As a rule, benign tumors do not metastasize. However, even this fundamental aspect of cancer biology has not gone unchallenged [195, 196]. Thus, it seems that while tumor progression and metastasis may coincide, the ability of neoplastic cells to disseminate and colonize new sites is determined by its own

unique biology. This biology of metastasis is not *de novo*, but borrowed and corrupted from normal physiological processes.

Cancer is by definition a disease of multicellular organisms. That is, cells which “cheat” the organism by prioritizing their own survival above that of the organism exploit host resources [197]. As metastasis is the spread of neoplastic cells from a primary tumor to a secondary site and growth therein, by definition there exist several requirements of organisms for metastasis to occur: 1) the organisms must get cancer and therefore must also be multicellular 2) the organisms must have different tissues large enough to permit colonization of the tumor cells in a region spatially distinct from the primary tumor and 3) the metastatic niche must permit growth of the disseminated cells. Thus, the study of metastasis is generally limited to multicellular eukaryotes. While biofilms and aggregates do occur in Bacteria and Archea, these lack sufficient intercellular adhesion, dependency and differentiation to be considered a true multicellular organism. Examples of true multicellular differentiation and dependency do exist in Bacteria [198], but these aggregates lack rogue cells which independently exploit the colony in the same way neoplastic cells do.

Turning to multicellular eukarotes, *Volvox* are a genus of algae which can experience a condition similar to cancer when genes which inhibit cell proliferation in somatic cells are not correctly expressed [199]. *Volvox* are comprised of a ball of cells differentiated into two distinct types: the majority of the cells are postmitotic, “somatic” flagella-containing cells on the exterior of the sphere while a smaller number of germ cells with the potential for proliferation exist in the center of the sphere [200]. The flagellated cells rely on the germ cells for regeneration and reproduction, while the germ cells rely

on the flagellates to move the organism to toward the light for photosynthesis and energy production. However, when the gene regA is not expressed in the outer somatic cells, they re-enter the cell cycle and resulting proliferative masses form new organisms [201]. In *Volvox*, nutrient deprivation and other environmental stresses cause the formation of reactive oxygen species (ROS). Sexual reproduction in *Volvox* has been correlated with increasing levels of ROS, leading to the hypothesis that sexual reproduction might promote survival in the face of environmental stress [202]. The same genes triggered during sexual reproduction of this organism are also triggered in response to wounding [203]. These parallel pathways of wound healing and coordinated cell proliferation are also seen in human cancer [204], illustrating striking parallels in biology. As yet though, invasion and metastasis of dysregulated *Volvox* cells has not been observed.

To truly observe metastasis then, we turn to multicellular animals. One of the simplest phyla for which disseminated cancer has been observed is Mollusca (mollusks), containing bivalve species like clams and mussels [205]. In soft shell clams, primary gonadal tumors have been observed in the gonad region of the clam and invading surrounding tissues [206]. Colonization of distant organs such as the gills is apparent, but given the large size of the primary tumor and proximity of the tumor to the gill, it remains possible that this represents an extension of local invasion rather than a true metastasis. Models of metastasis in *Drosophila* have been genetically engineered by expressing mutant oncogenes and/or inactivating tumor suppressors. $Ras^{V12}/scrib^{-/-}$ flies develop uncontrolled proliferation of developing eye-disc epithelial cells that subsequently leave the primary site and migrate throughout the developing larvae causing death before adulthood [207].

While the presentation of cancer may differ between species, often the genes regulating cancer progression and metastasis do not. So then, if we assume that genes selected for or against during cancer progression and metastasis have a defined role in normal physiology, primitive model systems with shared genetic history might provide valuable insight into the function and regulation of these genes, including the metastasis suppressors. While yet relatively unexplored, such model systems may help elucidate the molecular mechanism of these genes and provide a platform for pharmacologic screens that could be used to develop new treatments for disseminated and metastatic cancer.

There remains a critical need for metastasis research, as disseminated disease is a consistent indicator of poor prognosis for patients affected by cancer. Current and future treatments like surgery, radiation, conventional chemotherapy and targeted therapy will continue to affect the growth of cancer which has spread to other regions of the body. Metastasis itself however, may present its own therapeutic avenue that would be effective at several levels. Understanding the biology of metastasis holds great potential scientifically and therapeutically and holds promise and hope for the current and future patients affected by the spread of their cancer.

References

1. Siegel RL, Miller KD, Jemal A. Cancer statistics, 2018. CA Cancer J Clin 2018;68(1):7-30.
2. Steeg PS. Search for metastasis suppressor genes. Invasion Metastasis 1989;9(6):351-9.
3. Trevors JT, Saier MH. Three Laws of Biology. Water, Air, and Soil Pollution 2010;205(1):87-89.
4. Young ED, Li L, Behbod F*, et al.* Fundamental Relationships Between Cancer Stem Cells, the Cancer Stem Cell Niche and Metastasis. 2016.
5. Virchow R. Cellular-pathologie. Virchows Archiv 1855;8(1):3-39.
6. Durante F. Nesso fisio-patologico tra la struttura dei nei materni e la gentsi di alcuni tumori maligni. Arch Memor Observ Chir Prat 1874;11(217).
7. Cohnheim J. Congenitales, quergestreiftes Muskelsarkon der Nireren. Virchows Arch 1875; 65(64).
8. Osella-Abate S, Ribero S, Sanlorenzo M*, et al.* Risk factors related to late metastases in 1,372 melanoma patients disease free more than 10 years. Int. J. Cancer 2014; 10.1002/ijc.29281 [doi].
9. Patrick V, Tim CS, Shivkumar V*, et al.* Hematopoietic Stem Cell Quiescence Is Maintained by Compound Contributions of the Retinoblastoma Gene Family. Cell Stem Cell 2008;3(4):416-428.
10. Cotsarelis G, Sun TT, Lavker RM. Label-retaining cells reside in the bulge area of pilosebaceous unit: implications for follicular stem cells, hair cycle, and skin carcinogenesis. Cell 1990;61(7):1329-37.
11. Li L, Clevers H. Coexistence of quiescent and active adult stem cells in mammals. Science 2010;327(5965):542-5.
12. Necas E, Neuwirt J. Effect of hydroxyurea and vinblastine on the proliferation of the pluripotential stem cells. Neoplasma 1977;24(1):29-40.
13. Richichi C, Brescia P, Alberizzi V*, et al.* Marker-independent method for isolating slow-dividing cancer stem cells in human glioblastoma. Neoplasia 2013;15(7):840-7.
14. Eccles SA, Welch DR. Metastasis: recent discoveries and novel treatment strategies. Lancet 2007;369(9574):1742-1757.
15. Fidler IJ. Metastasis: guantitative analysis of distribution and fate of tumor embolilabeled with 125 I-5-iodo-2'-deoxyuridine. J Natl Cancer Inst 1970;45(4):773-82.
16. Miele ME, Robertson G, Lee JH*, et al.* Metastasis suppressed, but tumorigenicity and local invasiveness unaffected, in the human melanoma cell line MelJuSo after introduction of human chromosomes 1 or 6. Molecular carcinogenesis 1996;15(4):284-299.
17. Lee JH, Miele ME, Hicks DJ*, et al.* KiSS-1, a novel human malignant melanoma metastasis-suppressor gene. Journal of the National Cancer Institute 1996;88(23):1731-1737.
18. Lee JH, Welch DR. Suppression of metastasis in human breast carcinoma MDA-MB-435 cells after transfection with the metastasis suppressor gene, KiSS-1. Cancer research 1997;57(12):2384-2387.
19. Tagashira H, Hamazaki K, Tanaka N*, et al.* Reduced metastatic potential and c-myc overexpression of colon adenocarcinoma cells (Colon 26 line) transfected with

nm23-R2/rat nucleoside diphosphate kinase alpha isoform. Int J Mol Med 1998;2(1):65-8.
20. Miyazaki H, Fukuda M, Ishijima Y*, et al.* Overexpression of nm23-H2/NDP kinase B in a human oral squamous cell carcinoma cell line results in reduced metastasis, differentiated phenotype in the metastatic site, and growth factor-independent proliferative activity in culture. Clin Cancer Res 1999;5(12):4301-7.
21. Dong JT, Lamb PW, Rinker-Schaeffer CW*, et al.* KAI1, a metastasis suppressor gene for prostate cancer on human chromosome 11p11.2. Science 1995;268(5212):884-6.
22. Yamada SD, Hickson JA, Hrobowski Y*, et al.* Mitogen-activated protein kinase kinase 4 (MKK4) acts as a metastasis suppressor gene in human ovarian carcinoma. Cancer Res 2002;62(22):6717-23.
23. Gildea JJ, Seraj MJ, Oxford G*, et al.* RhoGDI2 is an invasion and metastasis suppressor gene in human cancer. Cancer Res 2002;62(22):6418-23.
24. Kurahara H, Bohl C, Natsugoe S*, et al.* Suppression of pancreatic cancer growth and metastasis by HMP19 identified through genome-wide shRNA screen. Int J Cancer 2016;139(3):628-38.
25. Khan I, Steeg PS. Metastasis suppressors: functional pathways. Lab Invest 2017; 10.1038/labinvest.2017.104.
26. Steeg PS, Bevilacqua G, Kopper L*, et al.* Evidence for a novel gene associated with low tumor metastatic potential. J Natl Cancer Inst 1988;80(3):200-4.
27. Goldberg SF, Harms JF, Quon K*, et al.* Metastasis-suppressed C8161 melanoma cells arrest in lung but fail to proliferate. Clinical & experimental metastasis 1999;17(7):601-607.
28. Nash KT, Phadke PA, Navenot JM*, et al.* Requirement of KISS1 secretion for multiple organ metastasis suppression and maintenance of tumor dormancy. J Natl Cancer Inst 2007;99(4):309-21.
29. Sasaki K, Kurahara H, Young ED*, et al.* Genome-wide in vivo RNAi screen identifies ITIH5 as a metastasis suppressor in pancreatic cancer. Clinical & Experimental Metastasis 2017; 10.1007/s10585-017-9840-3:1-11.
30. Fidler IJ. Selection of successive tumour lines for metastasis. Nature: New biology 1973;242(118):148-149.
31. Cowan FM, Klein DL, Armstrong GR*, et al.* Inhibition of rat adenocarcinoma metastases by "Staphylococcus aureus" protein A. Biomed Pharmacother 1982;36(1):29-31.
32. Freise CE, Liu T, Ascher NL*, et al.* Hepatotoxins and liver transplantation decrease pulmonary metastases in rats with hepatoma. J Surg Res 1996;64(2):198-202.
33. Chishima T, Miyagi Y, Wang X*, et al.* Cancer invasion and micrometastasis visualized in live tissue by green fluorescent protein expression. Cancer Res 1997;57(10):2042-7.
34. Zhang L, Hellstrom KE, Chen L. Luciferase activity as a marker of tumor burden and as an indicator of tumor response to antineoplastic therapy in vivo. Clin Exp Metastasis 1994;12(2):87-92.
35. Hoffman RM. Visualization of GFP-expressing tumors and metastasis in vivo. Biotechniques 2001;30(5):1016-22, 1024-6.

36. Mendoza A, Hong SH, Osborne T*, et al.* Modeling metastasis biology and therapy in real time in the mouse lung. J Clin Invest 2010;120(8):2979-88.
37. Damsky WE, Theodosakis N, Bosenberg M. Melanoma metastasis: new concepts and evolving paradigms. Oncogene 2014;33(19):2413-2422.
38. Yachida S, Iacobuzio-Donahue CA. The pathology and genetics of metastatic pancreatic cancer. Arch Pathol Lab Med 2009;133(3):413-22.
39. Box GEP. Robustness in the Strategy of Scientific Model Building A2 - LAUNER, ROBERT L. In: Wilkinson GN, (ed). *Robustness in Statistics*: Academic Press; 1979, 201-236.
40. Morgagni G. *Jo. Baptistae Morgagni P.P.P.P. De sedibus, et causis morborum per anatomen indagatis, libri quinque : dissectiones, et animadversiones, nunc primum editas, complectuntur propemodum innumeras, medicis, chirurgis, anatomicis profuturas : multiplex praefixus est index rerum, & nominum accuratissimus*. Edito secunda / ed. Patavii: Sumptibus Remondinianis; 1765.
41. Rogers GS. Narrow versus wide margins in malignant melanoma. J Dermatol Surg Oncol 1989;15(1):33-4.
42. Wolchok JD, Chiarion-Sileni V, Gonzalez R*, et al.* Overall Survival with Combined Nivolumab and Ipilimumab in Advanced Melanoma. N Engl J Med 2017;377(14):1345-1356.
43. Glenn F, Thorbjarnarson B. Carcinoma of the Pancreas. Ann Surg 1964;159:945-58.
44. Moore PS, Sipos B, Orlandini S*, et al.* Genetic profile of 22 pancreatic carcinoma cell lines. Analysis of K-ras, p53, p16 and DPC4/Smad4. Virchows Arch 2001;439(6):798-802.
45. Bardeesy N, DePinho RA. Pancreatic cancer biology and genetics. Nat Rev Cancer 2002;2(12):897-909.
46. Makohon-Moore AP, Zhang M, Reiter JG*, et al.* Limited heterogeneity of known driver gene mutations among the metastases of individual patients with pancreatic cancer. Nat Genet 2017;49(3):358-366.
47. Suter CM, Boffelli D, Martin DI. A role for epigenetic inheritance in modern evolutionary theory? A comment in response to Dickins and Rahman. Proc Biol Sci 2013;280(1771):20130903; discussion 20131820.
48. McDonald OG, Li X, Saunders T*, et al.* Epigenomic reprogramming during pancreatic cancer progression links anabolic glucose metabolism to distant metastasis. Nat Genet 2017;49(3):367-376.
49. Holliday R. DNA methylation and epigenetic mechanisms. Cell Biophys 1989;15(1-2):15-20.
50. Roe JS, Hwang CI, Somerville TDD*, et al.* Enhancer Reprogramming Promotes Pancreatic Cancer Metastasis. Cell 2017;170(5):875-888 e20.
51. p53/p16-Independent Epigenetic Therapy With Oral Decitabine/Tetrahydrouridine for Pancreatic Cancer. In: https://ClinicalTrials.gov/show/NCT02847000.
52. A Phase II Trial to Improve Outcomes in Patients With Resected Pancreatic Cancer (Azacitidine, Abraxane, Gemcitabine). In: https://ClinicalTrials.gov/show/NCT01845805.
53. Steinbuch M, Loeb J. Isolation of an alpha2-globulin from human plasma. Nature 1961;192:1196.

54. Himmelfarb M, Klopocki E, Grube S*, et al.* ITIH5, a novel member of the inter-alpha-trypsin inhibitor heavy chain family is downregulated in breast cancer. Cancer Letters 2004;204(1):69-77.
55. Chan P, Risler JL, Raguenez G*, et al.* The three heavy-chain precursors for the inter-alpha-inhibitor family in mouse: new members of the multicopper oxidase protein group with differential transcription in liver and brain. Biochem J 1995;306 (Pt 2):505-12.
56. Huang L, Yoneda M, Kimata K. A serum-derived hyaluronan-associated protein (SHAP) is the heavy chain of the inter alpha-trypsin inhibitor. J Biol Chem 1993;268(35):26725-30.
57. Hennies HC. All is balanced: inter-alpha-trypsin inhibitors as unseen extracellular matrix proteins in epidermal morphology and differentiation. Exp Dermatol 2015;24(9):661-2.
58. Huth S, Heise R, Vetter-Kauczok CS*, et al.* Inter-alpha-trypsin inhibitor heavy chain 5 (ITIH5) is overexpressed in inflammatory skin diseases and affects epidermal morphology in constitutive knockout mice and murine 3D-skin models. Exp. Dermatol 2015; 10.1111/exd.12704 [doi].
59. Hamm A, Veeck J, Bektas N*, et al.* Frequent expression loss of Inter-alpha-trypsin inhibitor heavy chain (ITIH) genes in multiple human solid tumors: a systematic expression analysis. BMC Cancer 2008;8:25.
60. Kloten V, Becker B, Winner K*, et al.* Promoter hypermethylation of the tumor-suppressor genes ITIH5, DKK3, and RASSF1A as novel biomarkers for blood-based breast cancer screening. Breast Cancer Res 2013;15(1):R4.
61. Rose M, Gaisa NT, Antony P*, et al.* Epigenetic inactivation of ITIH5 promotes bladder cancer progression and predicts early relapse of pT1 high-grade urothelial tumours. Carcinogenesis 2014;35(3):727-36.
62. Dotsch MM, Kloten V, Schlensog M*, et al.* Low expression of ITIH5 in adenocarcinoma of the lung is associated with unfavorable patients' outcome. Epigenetics 2015;10(10):903-12.
63. Zhang S, Feng XL, Shi L*, et al.* Genome-wide analysis of DNA methylation in tongue squamous cell carcinoma. Oncol Rep 2013;29(5):1819-26.
64. Perez-Ramirez M, Hernandez-Jimenez AJ, Guerrero-Guerrero A*, et al.* Genomics and epigenetics: A study of ependymomas in pediatric patients. Clin Neurol Neurosurg 2016;144:53-8.
65. Oing C, Jost E, Dahl E*, et al.* Aberrant DNA hypermethylation of the ITIH5 tumor suppressor gene in acute myeloid leukemia. Clin Epigenetics 2011;2(2):419-23.
66. Mai C, Zhao JJ, Tang XF*, et al.* Decreased ITIH5 expression is associated with poor prognosis in primary gastric cancer. Med. Oncol 2014;31(7):53.
67. Pita JM, Banito A, Cavaco BM*, et al.* Gene expression profiling associated with the progression to poorly differentiated thyroid carcinomas. Br J Cancer 2009;101(10):1782-91.
68. Rose M, Kloten V, Noetzel E*, et al.* ITIH5 mediates epigenetic reprogramming of breast cancer cells. Mol Cancer 2017;16(1):44.
69. Rose M, Meurer SK, Kloten V*, et al.* ITIH5 induces a shift in TGF-beta superfamily signaling involving Endoglin and reduces risk for breast cancer metastasis and tumor death. Mol Carcinog 2018;57(2):167-181.

70. Askanazy M. Die Teratome nach ihrem Bau, ihrem Verlauf, ihrer Genese and im Vergleich zum experimentellen Teratoid. Verhandlungen der Deutschen Pathologischen Gesellschaft 1907;11:39–82.
71. Damjanov I, Solter D. Experimental teratoma. Curr Top Pathol 1974;59:69-130.
72. Kleinsmith LJ, Pierce GB. Multipotentiality of single embryonal carcinoma cells. Multipotentiality of single embryonal carcinoma cells 1964, http://scholar.google.com/scholar?q=Multipotentiality of single embryonal carcinoma cells&btnG=&hl=en&num=20&as_sdt=0%2C22.
73. Furth J, Kahn MC, Breedis C. The transmission of leukemia of mice with a single cell. The American Journal of Cancer 1937, http://cancerres.aacrjournals.org/content/amjcancer/31/2/276.abstract.
74. Lapidot T, Sirard C, Vormoor J*, et al.* A Cell Initiating Human Acute Myeloid-Leukemia After Transplantation Into Scid Mice. Nature 1994;367(6464):645-648.
75. Pierce GB, Wallace C. Differentiation of malignant to benign cells. Cancer research 1971;31(2):127-134.
76. Chen J, Li Y, Yu TS*, et al.* A restricted cell population propagates glioblastoma growth after chemotherapy. Nature 2012;488(7412):522-6.
77. Schepers AG, Snippert HJ, Stange DE*, et al.* Lineage tracing reveals Lgr5+ stem cell activity in mouse intestinal adenomas. Science 2012;337(6095):730-5.
78. Nowell PC. The clonal evolution of tumor cell populations. Science 1976;194(4260):23-8.
79. Dear TN, Kefford RF. Molecular oncogenetics of metastasis. Molecular aspects of medicine 1989;11(4):243-324.
80. Guo W, Keckesova Z, Donaher JL*, et al.* Slug and Sox9 cooperatively determine the mammary stem cell state. Cell 2012;148(5):1015-28.
81. Al-Hajj M, Wicha MS, Benito-Hernandez A*, et al.* Prospective identification of tumorigenic breast cancer cells. Proceedings of the National Academy of Sciences of the United States of America 2003;100(7):3983-3988.
82. François V, Marie-Liesse LA-L, Mark S*, et al.* The mammary progenitor marker CD61/beta3 integrin identifies cancer stem cells in mouse models of mammary tumorigenesis. Cancer research 2008;68(19):7711-7717.
83. Chen MS, Woodward WA, Behbod F*, et al.* Wnt/beta-catenin mediates radiation resistance of Sca1+ progenitors in an immortalized mammary gland cell line. J Cell Sci 2007;120(Pt 3):468-77.
84. Canesin G, Cuevas EP, Santos V*, et al.* Lysyl oxidase-like 2 (LOXL2) and E47 EMT factor: novel partners in E-cadherin repression and early metastasis colonization. Oncogene 2015;34(8):951-64.
85. Kantara C, O'Connell MR, Luthra G*, et al.* Methods for detecting circulating cancer stem cells (CCSCs) as a novel approach for diagnosis of colon cancer relapse/metastasis. Lab Invest 2015;95(1):100-12.
86. Ocana OH, Corcoles R, Fabra A*, et al.* Metastatic colonization requires the repression of the epithelial-mesenchymal transition inducer Prrx1. Cancer Cell 2012;22(6):709-24.
87. Chaffer CL, Thompson EW, Williams ED. Mesenchymal to epithelial transition in development and disease. Cells Tissues Organs 2007;185(1-3):7-19.

88. Cheung M, Chaboissier MC, Mynett A*, et al.* The transcriptional control of trunk neural crest induction, survival, and delamination. The transcriptional control of trunk neural crest induction, survival, and delamination 2005, http://scholar.google.com/scholar?q=The transcriptional control of trunk neural crest induction, survival, and delamination&btnG=&hl=en&num=20&as_sdt=0%2C22.
89. Jianqun L, Feng Q, Nana T*, et al.* Ovarian Cancer Spheroid Cells with Stem Cell-Like Properties Contribute to Tumor Generation, Metastasis and Chemotherapy Resistance through Hypoxia-Resistant Metabolism. PloS one 2013;9(1).
90. Brabletz T, Hlubek F, Spaderna S*, et al.* Invasion and metastasis in colorectal cancer: epithelial-mesenchymal transition, mesenchymal-epithelial transition, stem cells and beta-catenin. Cells Tissues Organs 2005;179(1-2):56-65.
91. Colombo C, Foo WC, Whiting D*, et al.* FAP-related desmoid tumors: a series of 44 patients evaluated in a cancer referral center. Histology and histopathology 2012;27(5):641-649.
92. Zhou G, Wang J, Zhao M*, et al.* Gain-of-Function Mutant p53 Promotes Cell Growth and Cancer Cell Metabolism via Inhibition of AMPK Activation. Molecular cell 2014;54(6):960-974.
93. Ciavardelli D, Rossi C, Barcaroli D*, et al.* Breast cancer stem cells rely on fermentative glycolysis and are sensitive to 2-deoxyglucose treatment. Cell death & disease 2013;5.
94. Liu W, Beck BH, Vaidya KS*, et al.* Metastasis suppressor KISS1 seems to reverse the Warburg effect by enhancing mitochondrial biogenesis. Cancer research 2014;74(3):954-963.
95. Schofield R. The relationship between the spleen colony-forming cell and the haemopoietic stem cell. Blood cells 1977;4(1-2):7-25.
96. Folkins C, Man S, Xu P*, et al.* Anticancer therapies combining antiangiogenic and tumor cell cytotoxic effects reduce the tumor stem-like cell fraction in glioma xenograft tumors. Cancer research 2007;67(8):3560-3564.
97. Kaplan RN, Psaila B, Lyden D. Bone marrow cells in the 'pre-metastatic niche': within bone and beyond. Cancer metastasis reviews 2006;25(4):521-529.
98. Goodman LS, Wintrobe MM. Nitrogen mustard therapy; use of methyl-bis (beta-chloroethyl) amine hydrochloride and tris (beta-chloroethyl) amine hydrochloride for Hodgkin's disease, lymphosarcoma, leukemia and certain allied and miscellaneous disorders. Journal of the American Medical Association 1946;132:126-132.
99. Flesken-Nikitin A, Hwang C-II, Cheng C-YY*, et al.* Ovarian surface epithelium at the junction area contains a cancer-prone stem cell niche. Nature 2013;495(7440):241-245.
100. Chen J, Li Y, Yu TS*, et al.* A restricted cell population propagates glioblastoma growth after chemotherapy. Nature 2012;488(7412):522-526.
101. Schepers AG, Snippert HJ, Stange DE*, et al.* Lineage tracing reveals Lgr5+ stem cell activity in mouse intestinal adenomas. Science 2012;337(6095):730-735.
102. Hwang RF, Moore T, Arumugam T*, et al.* Cancer-associated stromal fibroblasts promote pancreatic tumor progression. Cancer research 2008;68(3):918-926.
103. Xu Z, Vonlaufen A, Phillips PA*, et al.* Role of pancreatic stellate cells in pancreatic cancer metastasis. The American journal of pathology 2010;177(5):2585-2596.

104. Knelson EH, Gaviglio AL, Nee JC*, et al.* Stromal heparan sulfate differentiates neuroblasts to suppress neuroblastoma growth. J. Clin. Invest 2014;124(7):3016-3031.
105. Knelson EH, Gaviglio AL, Tewari AK*, et al.* Type III TGF-β receptor promotes FGF2-mediated neuronal differentiation in neuroblastoma. The Journal of clinical investigation 2013;123(11):4786-4798.
106. Vaillant F, Asselin-Labat M-LL, Shackleton M*, et al.* The mammary progenitor marker CD61/beta3 integrin identifies cancer stem cells in mouse models of mammary tumorigenesis. Cancer research 2008;68(19):7711-7717.
107. Singh SK, Clarke ID, Terasaki M*, et al.* Identification of a cancer stem cell in human brain tumors. Cancer research 2003;63(18):5821-5828.
108. Kozovska Z, Gabrisova V, Kucerova L. Colon cancer: Cancer stem cells markers, drug resistance and treatment. Biomedicine & pharmacotherapy = Biomedecine & pharmacotherapie 2014; 10.1016/j.biopha.2014.10.019.
109. Baggiolini A, Varum S, Mateos JM*, et al.* Premigratory and migratory neural crest cells are multipotent in vivo. Cell Stem Cell 2015;16(3):314-22.
110. Gupta PB, Kuperwasser C, Brunet J-PP*, et al.* The melanocyte differentiation program predisposes to metastasis after neoplastic transformation. Nature genetics 2005;37(10):1047-1054.
111. Warburg O, Wind F, Negelein E. The metabolism of tumors in the body. Journal of General Physiology 1927;8(6):519-530.
112. Ciavardelli D, Rossi C, Barcaroli D*, et al.* Breast cancer stem cells rely on fermentative glycolysis and are sensitive to 2-deoxyglucose treatment. Cell Death. Dis 2014;5:e1336.
113. Kocabas F, Zheng J, Zhang C*, et al.* Metabolic Characterization of Hematopoietic Stem Cells. In: Bunting KD, Qu C-K, (eds). *Hematopoietic Stem Cell Protocols*: Springer New York; 2014, 155-164.
114. Takubo K, Nagamatsu G, Kobayashi CI*, et al.* Regulation of glycolysis by Pdk functions as a metabolic checkpoint for cell cycle quiescence in hematopoietic stem cells. Cell Stem Cell 2013;12(1):49-61.
115. Liu W, Beck BH, Vaidya KS*, et al.* Metastasis suppressor KISS1 seems to reverse the Warburg effect by enhancing mitochondrial biogenesis. Cancer Res 2014;74(3):954-963.
116. Wang Y-HH, Israelsen WJ, Lee D*, et al.* Cell-state-specific metabolic dependency in hematopoiesis and leukemogenesis. Cell 2014;158(6):1309-1323.
117. Crocetti E, Paci E. Malignant carcinoids in the USA, SEER 1992-1999. An epidemiological study with 6830 cases. European journal of cancer prevention : the official journal of the European Cancer Prevention Organisation (ECP) 2003;12(3):191-194.
118. Levy AD, Sobin LH. From the archives of the AFIP: Gastrointestinal carcinoids: imaging features with clinicopathologic comparison. Radiographics : a review publication of the Radiological Society of North America, Inc 2006;27(1):237-257.
119. Bleul CC, Fuhlbrigge RC, Casasnovas JM*, et al.* A highly efficacious lymphocyte chemoattractant, stromal cell-derived factor 1 (SDF-1). The Journal of experimental medicine 1996;184(3):1101-1109.

120. Lévesque J-PP, Hendy J, Takamatsu Y*, et al.* Disruption of the CXCR4/CXCL12 chemotactic interaction during hematopoietic stem cell mobilization induced by GCSF or cyclophosphamide. The Journal of clinical investigation 2002;111(2):187-196.
121. Muller A, Homey B, Soto H*, et al.* Involvement of chemokine receptors in breast cancer metastasis. Nature 2001;410(6824):50-6.
122. DeCastro AJ, Cherukuri P, Balboni A*, et al.* ΔNP63α Transcriptionally Activates Chemokine Receptor 4 (CXCR4) Expression to Regulate Breast Cancer Stem Cell Activity and Chemotaxis. Molecular cancer therapeutics 2014; 10.1158/1535-7163.MCT-14-0194.
123. Mani SA, Guo W, Liao MJ*, et al.* The epithelial-mesenchymal transition generates cells with properties of stem cells. Cell 2008, http://www.sciencedirect.com/science/article/pii/S0092867408004443.
124. Jing Y, Sendurai AM, Joana LD*, et al.* Twist, a master regulator of morphogenesis, plays an essential role in tumor metastasis. Cell 2004;117(7):927-939.
125. Marie-Egyptienne DT, Lohse I, Hill RP. Cancer stem cells, the epithelial to mesenchymal transition (EMT) and radioresistance: potential role of hypoxia. Cancer Lett 2013;341(1):63-72.
126. Mujcic H, Hill RP, Koritzinsky M*, et al.* Hypoxia signaling and the metastatic phenotype. Curr Mol Med 2014;14(5):565-79.
127. Tarin D, Thompson EW, Newgreen DF. The fallacy of epithelial mesenchymal transition in neoplasia. Cancer Res 2005;65(14):5996-6000; discussion 6000-1.
128. Liu S, Dontu G, Mantle ID*, et al.* Hedgehog signaling and Bmi-1 regulate self-renewal of normal and malignant human mammary stem cells. Hedgehog signaling and Bmi-1 regulate self-renewal of normal and malignant human mammary stem cells 2006; 10.1158/0008-5472.CAN-06-0054.
129. Maynard MA, Ferretti R, Hilgendorf KI*, et al.* Bmi1 is required for tumorigenesis in a mouse model of intestinal cancer. Oncogene 2014;33(28):3742-7.
130. Hartwell KA, Muir B, Reinhardt F*, et al.* The Spemann organizer gene, Goosecoid, promotes tumor metastasis. Proc Natl Acad Sci U S A 2006;103(50):18969-74.
131. Weygant N, Qu D, May R*, et al.* DCLK1 is a broadly dysregulated target against epithelial-mesenchymal transition, focal adhesion, and stemness in clear cell renal carcinoma. Oncotarget 2015;6(4):2193-205.
132. Li L, Xie T. Stem cell niche: structure and function. Annual review of cell and developmental biology 2004;21:605-631.
133. Li L, Neaves WB. Normal stem cells and cancer stem cells: the niche matters. Cancer Res 2006;66(9):4553-7.
134. Borovski T, De Sousa EMF, Vermeulen L*, et al.* Cancer stem cell niche: the place to be. Cancer Res 2011;71(3):634-9.
135. Hovinga KE, Shimizu F, Wang R*, et al.* Inhibition of notch signaling in glioblastoma targets cancer stem cells via an endothelial cell intermediate. Stem cells (Dayton, Ohio) 2010;28(6):1019-1029.
136. Kaplan RN, Psaila B, Lyden D. Niche-to-niche migration of bone-marrow-derived cells. Trends in molecular medicine 2007;13(2):72-81.

137. Kaplan RN, Riba RD, Zacharoulis S*, et al.* VEGFR1-positive haematopoietic bone marrow progenitors initiate the pre-metastatic niche. Nature 2005;438(7069):820-827.
138. Wang H, Yu C, Gao X*, et al.* The osteogenic niche promotes early-stage bone colonization of disseminated breast cancer cells. Cancer Cell 2015;27(2):193-210.
139. Peinado H, Aleckovic M, Lavotshkin S*, et al.* Melanoma exosomes educate bone marrow progenitor cells toward a pro-metastatic phenotype through MET. Nat Med 2012;18(6):883-91.
140. Brown R, Curry E, Magnani L*, et al.* Poised epigenetic states and acquired drug resistance in cancer. Nat Rev Cancer 2014;14(11):747-53.
141. Young ED, Strom K, Tsue AF*, et al.* Automated quantitative image analysis for ex vivo metastasis assays reveals differing lung composition requirements for metastasis suppression by KISS1. Clinical & Experimental Metastasis 2018; 10.1007/s10585-018-9882-1.
142. Heller D, Hoppe A, Restrepo S*, et al.* EpiTools: An Open-Source Image Analysis Toolkit for Quantifying Epithelial Growth Dynamics. Dev Cell 2016;36(1):103-116.
143. Li C, Guo J, Cong R*, et al.* Underwater Image Enhancement by Dehazing with Minimum Information Loss and Histogram Distribution Prior. IEEE Trans Image Process 2016; 10.1109/TIP.2016.2612882.
144. Henriquez NV, van Overveld PG, Que I*, et al.* Advances in optical imaging and novel model systems for cancer metastasis research. Clin Exp Metastasis 2007;24(8):699-705.
145. Phillips KG, Baker-Groberg SM, McCarty OJ. Quantitative optical microscopy: measurement of cellular biophysical features with a standard optical microscope. J Vis Exp 2014; 10.3791/50988(86).
146. Mendoza A, Hong S-HH, Osborne T*, et al.* Modeling metastasis biology and therapy in real time in the mouse lung. The Journal of clinical investigation 2010;120(8):2979-2988.
147. Michael M. Lizardo PHS. Practical Considerations in Studying Metastatic Lung Colonization in Osteosarcoma Using the Pulmonary Metastasis Assay. Journal of Visualized Experiments 2017, https://www.jove.com/video/56332/practical-considerations-studying-metastatic-lung-colonization.
148. Keyvani A, Kyle S. A fully-automated image processing technique to improve measurement of suspended particles and flocs by removing out-of-focus objects. Computers & Geosciences 2013;52:189198.
149. Beck BH, Welch DR. The KISS1 metastasis suppressor: a good night kiss for disseminated cancer cells. European journal of cancer (Oxford, England : 1990) 2010;46(7):1283-1289.
150. Welch DR, Chen P, Miele ME*, et al.* Microcell-mediated transfer of chromosome 6 into metastatic human C8161 melanoma cells suppresses metastasis but does not inhibit tumorigenicity. Oncogene 1993;9(1):255-262.
151. Nash KT, Phadke PA, Navenot J-MM*, et al.* Requirement of KISS1 secretion for multiple organ metastasis suppression and maintenance of tumor dormancy. Journal of the National Cancer Institute 2007;99(4):309-321.
152. Schneider CA, Rasband WS, Eliceiri KW. NIH Image to ImageJ: 25 years of image analysis. Nat Methods 2012;9(7):671-5.

153. Siritantikorn S, Jintaworn S, Noisakran S*, et al.* Application of ImageJ program to the enumeration of Orientia tsutsugamushi organisms cultured in vitro. Trans R Soc Trop Med Hyg 2012;106(10):632-5.
154. R: A language and environment for statistical computing. 2015.
155. MATLAB. In. Natick, Massachusetts: The MathWorks Inc.; 2015.
156. Goldberg SF, Miele ME, Hatta N*, et al.* Melanoma metastasis suppression by chromosome 6: evidence for a pathway regulated by CRSP3 and TXNIP. Cancer research 2003;63(2):432-440.
157. Kimura H, Hayashi K, Yamauchi K*, et al.* Real-time imaging of single cancer-cell dynamics of lung metastasis. J Cell Biochem 2010;109(1):58-64.
158. Leong HS, Lizardo MM, Ablack A*, et al.* Imaging the impact of chemically inducible proteins on cellular dynamics in vivo. PLoS One 2012;7(1):e30177.
159. Hedberg-Buenz A, Christopher MA, Lewis CJ*, et al.* Quantitative measurement of retinal ganglion cell populations via histology-based random forest classification. Exp Eye Res 2016;146:370-85.
160. Jones TR, Carpenter AE, Lamprecht MR*, et al.* Scoring diverse cellular morphologies in image-based screens with iterative feedback and machine learning. Proc Natl Acad Sci U S A 2009;106(6):1826-31.
161. Lambert AW, Pattabiraman DR, Weinberg RA. Emerging Biological Principles of Metastasis. Cell 2017;168(4):670-691.
162. Chaffer CL, San Juan BP, Lim E*, et al.* EMT, cell plasticity and metastasis. Cancer Metastasis Rev 2016;35(4):645-654.
163. Jerome Friedman TH, Robert Tibshirani. Additive Logistic Regression: A Statistical View of Boosting. The Annals of Statistics 2000;28(2):337-407.
164. Angeliki M, Nikolaos P, Peter L*, et al.* The kisspeptin (KiSS-1)/GPR54 system in cancer biology. Cancer treatment reviews 2008;34(8):682-692.
165. Morcel K, Watrin T, Jaffre F*, et al.* Involvement of ITIH5, a candidate gene for congenital uterovaginal aplasia (Mayer-Rokitansky-Kuster-Hauser syndrome), in female genital tract development. Gene Expr 2012;15(5-6):207-14.
166. Kloten V, Rose M, Kaspar S*, et al.* Epigenetic inactivation of the novel candidate tumor suppressor gene ITIH5 in colon cancer predicts unfavorable overall survival in the CpG island methylator phenotype. Epigenetics 2014;9(9):1290-301.
167. Zhuo L, Kimata K. Structure and function of inter-alpha-trypsin inhibitor heavy chains. Connect Tissue Res 2008;49(5):311-20.
168. Baecker V. *ImageJ Macro Tool Sets for Biological Image Analysis*. http://dev.mri.cnrs.fr/projects/imagej-macros/wiki/Wound_Healing_Tool.
169. Thery C, Amigorena S, Raposo G*, et al.* Isolation and characterization of exosomes from cell culture supernatants and biological fluids. Curr Protoc Cell Biol 2006;Chapter 3:Unit 3 22.
170. Veeck J, Chorovicer M, Naami A*, et al.* The extracellular matrix protein ITIH5 is a novel prognostic marker in invasive node-negative breast cancer and its aberrant expression is caused by promoter hypermethylation. Oncogene 2008;27(6):865-876.
171. Barretina J, Caponigro G, Stransky N*, et al.* The Cancer Cell Line Encyclopedia enables predictive modelling of anticancer drug sensitivity. Nature 2012;483(7391):603-7.

172. Zhong Y, Macgregor-Das A, Saunders T*, et al.* Mutant p53 Together with TGFbeta Signaling Influence Organ-Specific Hematogenous Colonization Patterns of Pancreatic Cancer. Clin Cancer Res 2017;23(6):1607-1620.
173. Ridley AJ. Rho GTPase signalling in cell migration. Curr Opin Cell Biol 2015;36:103-12.
174. Lawson CD, Fan C, Mitin N*, et al.* Rho GTPase Transcriptome Analysis Reveals Oncogenic Roles for Rho GTPase-Activating Proteins in Basal-like Breast Cancers. Cancer Res 2016;76(13):3826-37.
175. Avraham H, Weinberg RA. Characterization and expression of the human rhoH12 gene product. Mol Cell Biol 1989;9(5):2058-66.
176. Bourguignon LY. Hyaluronan-mediated CD44 activation of RhoGTPase signaling and cytoskeleton function promotes tumor progression. Semin Cancer Biol 2008;18(4):251-9.
177. Culty M, Miyake K, Kincade PW*, et al.* The hyaluronate receptor is a member of the CD44 (H-CAM) family of cell surface glycoproteins. J Cell Biol 1990;111(6 Pt 1):2765-74.
178. Hou YC, Chao YJ, Tung HL*, et al.* Coexpression of CD44-positive/CD133-positive cancer stem cells and CD204-positive tumor-associated macrophages is a predictor of survival in pancreatic ductal adenocarcinoma. Cancer 2014;120(17):2766-77.
179. Bourguignon LY, Wong G, Earle C*, et al.* Hyaluronan-CD44 interaction promotes c-Src-mediated twist signaling, microRNA-10b expression, and RhoA/RhoC up-regulation, leading to Rho-kinase-associated cytoskeleton activation and breast tumor cell invasion. J Biol Chem 2010;285(47):36721-35.
180. Jessen TE, Odum L, Johnsen AH. In vivo binding of human inter-alpha-trypsin inhibitor free heavy chains to hyaluronic acid. Biol Chem Hoppe Seyler 1994;375(8):521-6.
181. Horm TM, Schroeder JA. MUC1 and metastatic cancer: expression, function and therapeutic targeting. Cell Adh Migr 2013;7(2):187-98.
182. Li C, Heidt DG, Dalerba P*, et al.* Identification of pancreatic cancer stem cells. Cancer Res 2007;67(3):1030-7.
183. Crist DW, Sitzmann JV, Cameron JL. Improved hospital morbidity, mortality, and survival after the Whipple procedure. Ann Surg 1987;206(3):358-65.
184. Bender RH, Haigis KM, Gutmann DH. Activated k-ras, but not h-ras or N-ras, regulates brain neural stem cell proliferation in a raf/rb-dependent manner. Stem Cells 2015;33(6):1998-2010.
185. Smit VT, Boot AJ, Smits AM*, et al.* KRAS codon 12 mutations occur very frequently in pancreatic adenocarcinomas. Nucleic Acids Res 1988;16(16):7773-82.
186. Gottsch ML, Cunningham MJ, Smith JT*, et al.* A role for kisspeptins in the regulation of gonadotropin secretion in the mouse. Endocrinology 2004;145(9):4073-7.
187. Havis E, Bonnin MA, Olivera-Martinez I*, et al.* Transcriptomic analysis of mouse limb tendon cells during development. Development 2014;141(19):3683-96.
188. Hauge-Evans AC, Richardson CC, Milne HM*, et al.* A role for kisspeptin in islet function. Diabetologia 2006;49(9):2131-5.
189. Reetz A, Solimena M, Matteoli M*, et al.* GABA and pancreatic beta-cells: colocalization of glutamic acid decarboxylase (GAD) and GABA with synaptic-like

microvesicles suggests their role in GABA storage and secretion. EMBO J 1991;10(5):1275-84.
190. Langley OK, Aletsee-Ufrecht MC, Grant NJ*, et al.* Expression of the neural cell adhesion molecule NCAM in endocrine cells. J Histochem Cytochem 1989;37(6):781-91.
191. Devaskar SU, Giddings SJ, Rajakumar PA*, et al.* Insulin gene expression and insulin synthesis in mammalian neuronal cells. J Biol Chem 1994;269(11):8445-54.
192. Arntfield ME, van der Kooy D. beta-Cell evolution: How the pancreas borrowed from the brain: The shared toolbox of genes expressed by neural and pancreatic endocrine cells may reflect their evolutionary relationship. Bioessays 2011;33(8):582-7.
193. Hanahan D, Weinberg RA. The hallmarks of cancer. Cell 2000;100(1):57-70.
194. Hanahan D, Weinberg RA. Hallmarks of cancer: the next generation. Cell 2011;144(5):646-674.
195. Anonymous. Metastasis of benign tumors. JAMA 1906;46(1):41.
196. Henske EP. Metastasis of benign tumor cells in tuberous sclerosis complex. Genes Chromosomes Cancer 2003;38(4):376-81.
197. Aktipis CA, Boddy AM, Jansen G*, et al.* Cancer across the tree of life: cooperation and cheating in multicellularity. Philos Trans R Soc Lond B Biol Sci 2015;370(1673).
198. Haselkorn R. Heterocysts. Annual Review of Plant Physiology and Plant Molecular Biology 1978;29:319-344.
199. Bonner JT. Volvox: Molecular-Genetic Origins of Multicellularity and Cellular Differentiation. David L. Kirk. The Quarterly Review of Biology 1998;73(4):506-506.
200. Miller SM. Volvox, Chlamydomonas, and the Evolution of Multicellularity. Nature Education 2010;3(9):65.
201. Kirk MM, Stark K, Miller SM*, et al.* regA, a Volvox gene that plays a central role in germ-soma differentiation, encodes a novel regulatory protein. Development 1999;126(4):639-647.
202. Nedelcu AM, Michod RE. Sex as a response to oxidative stress: the effect of antioxidants on sexual induction in a facultatively sexual lineage. Proceedings of the Royal Society B-Biological Sciences 2003;270:S136-S139.
203. Amon P, Haas E, Sumper M. The sex-inducing pheromone and wounding trigger the same set of genes in the multicellular green alga Volvox. Plant Cell 1998;10(5):781-789.
204. Arwert EN, Hoste E, Watt FM. Epithelial stem cells, wound healing and cancer. Nat Rev Cancer 2012;12(3):170-80.
205. Barber BJ. Neoplastic diseases of commercially important marine bivalves. Aquatic Living Resources 2004;17(4):449-466.
206. Yevich PP, Barszcz CA. Gonadal and Hematopoietic Neoplasms in Mya-Arenaria. Marine Fisheries Review 1976;38(10):42-43.
207. Pagliarini RA, Xu T. A genetic screen in Drosophila for metastatic behavior. Science 2003;302(5648):1227-31.